catalysts

MDPI

Review

Direct Synthesis of Dimethyl Ether from CO_2: Recent Advances in Bifunctional/Hybrid Catalytic Systems

Noelia Mota, Elena Millán Ordoñez, Bárbara Pawelec, José Luis G. Fierro and Rufino M. Navarro *

Instituto de Catálisis y Petroleoquímica, The Sustainable Energy and Chemistry Group, Consejo Superior de Investigaciones Científicas, 28049 Madrid, Spain; noelia.mota@icp.csic.es (N.M.); elena.millan.ordonez@csic.es (E.M.O.); bgarcia@icp.csic.es (B.P.); jlgfierro@icp.csic.es (J.L.G.F.)
* Correspondence: r.navarro@icp.csic.es; Tel.: +34-915854774

Abstract: Dimethyl ether (DME) is a versatile raw material and an interesting alternative fuel that can be produced by the catalytic direct hydrogenation of CO_2. Recently, this process has attracted the attention of the industry due to the environmental benefits of CO_2 elimination from the atmosphere and its lower operating costs with respect to the classical, two-step synthesis of DME from syngas ($CO + H_2$). However, due to kinetics and thermodynamic limits, the direct use of CO_2 as raw material for DME production requires the development of more effective catalysts. In this context, the objective of this review is to present the latest progress achieved in the synthesis of bifunctional/hybrid catalytic systems for the CO_2-to-DME process. For catalyst design, this process is challenging because it should combine metal and acid functionalities in the same catalyst, in a correct ratio and with controlled interaction. The metal catalyst is needed for the activation and transformation of the stable CO_2 molecules into methanol, whereas the acid catalyst is needed to dehydrate the methanol into DME. Recent developments in the catalyst design have been discussed and analyzed in this review, presenting the different strategies employed for the preparation of novel bifunctional catalysts (physical/mechanical mixing) and hybrid catalysts (co-precipitation, impregnation, etc.) with improved efficiency toward DME formation. Finally, an outline of future prospects for the research and development of efficient bi-functional/hybrid catalytic systems will be presented.

Keywords: CO_2 hydrogenation; dimethyl ether; DME; bifunctional catalyst; hybrid catalyst

Citation: Mota, N.; Millán Ordoñez, E.; Pawelec, B.; Fierro, J.L.G.; Navarro, R.M. Direct Synthesis of Dimethyl Ether from CO_2: Recent Advances in Bifunctional/Hybrid Catalytic Systems. *Catalysts* **2021**, *11*, 411. https://doi.org/10.3390/catal11040411

Academic Editor: Javier Ereña Loizaga

Received: 4 March 2021
Accepted: 22 March 2021
Published: 24 March 2021

1. Introduction

Despite the increasing use of renewable energy sources, fossil fuels (oil, coal, and natural gas) continue to be used in the short and medium term [1]. Unfortunately, the combustion of carbon-based fossil fuels is accompanied by huge emissions of CO_2 (in 2019, global energy-related CO_2 emissions reached around 33 gigatons (Gt)), disrupting the Earth's natural carbon cycle and causing global warming, ocean acidification, sea-level rise, and climate change [2]. Therefore, the use of fossil fuels in the near future should include their efficient transformation and the carbon capture and utilization (CCU) of the CO_2 produced. By way of example, the 2014 European Council committed EU member countries to achieve a national economy-wide target of at least a 40% reductions in greenhouse gas (GHG) emissions by 2030, which is in line with a cost-effective path of reducing at least 80% of greenhouse gas emissions by 2050 [3]

In addition to the challenges to achieve effective CO_2 capture, its use as raw material for the production of chemical building blocks and synthetic fuels is also a major technological challenge [4]. There are several C-rich chemical products that could be synthesized from CO_2 (Figure 1). However, the industrial use of CO_2 in the synthesis of chemicals is currently limited to a few processes, such as the synthesis of urea and its derivatives and the synthesis of salicylic acid and carbonates, with an annual consumption of CO_2 of around 140 MTm/year [5]. The conversion of CO_2 into chemicals can be achieved

through carboxylation reactions, where the CO_2 molecule is used as a precursor of organic compounds such as polymers, acrylates, and carbonates, or to produce methane, methanol, and urea through reactions where C-O bonds are broken [6–8]. CO_2 can be used also as raw material to obtain synthetic fuels via the Fischer–Tropsch process, direct dimethyl ether (DME), or methanol-to-gas/diesel. The CO_2-based fuels can offer benefits to achieve a more cost-effective energy transition in relation to full electrification alternatives, as demonstrated in the Study Integrated Energy Transition of the German Energy Agency [9], whose conclusions revealed that decarbonization scenarios based on a technology mix with CCU-CO_2 fuels (80–95% emissions reduction) can help reach climate targets at a lower cost than in the case of a full electrified scenario.

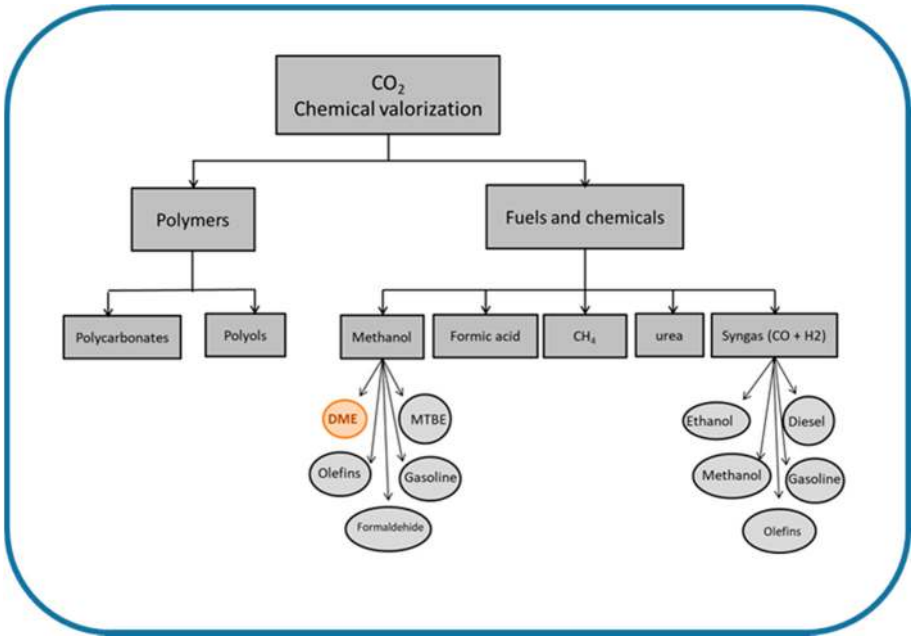

Figure 1. Main chemical valorization routes for CO_2 as feedstock.

DME is one of the most useful and versatile chemicals that can be produced from CO_2 (Figure 1) [10,11]. The global production of DME is relatively high (around 5 MTm per year) and is expected to grow steadily in the near future. The main market for DME is focused in Asia (85% of the world market) where DME is currently used as a clean fuel for residential use [12]. DME is also used as a refrigerant gas and is a key raw chemical for the production of methylation agents used to produce alkyl-aromatics, aerosol propellants, polishing products [13], dimethyl sulfate [13], methyl acetate [13], light olefins [14,15], aromatics, ethanol [16], and other important chemicals [17,18]. Another more recent interest of DME is related to its use as a "hydrogen carrier" for both storage and transportation of hydrogen through two coupled chemical processes: The synthesis of DME through CO_2 hydrogenation (H_2 storage) and the steam reforming of DME (H_2 production) [18].

DME is also a reliable alternative fuel for diesel engines because it exhibits a low steam saturation pressure, high calorific value (Table 1), similar cetane number (55–60), and good detonating properties (low ignition temperature). However, the lower heating value (LHV) of DME is much lower than that of conventional diesel (27.6 vs. 42.5 MJ/kg), and it exhibits low viscosity and solvent capacity. The advantages of dimethyl ether over conventional diesel include decreased emissions of NOx, hydrocarbons, and carbon monoxide, and its combustion does not produce soot [19]. Indeed, since 1995, DME has possessed the certification of California Ultra Low Emissions Vehicle (ULEV) of a nonpolluting ultra-clean fuel.

Table 1. Physicochemical properties of dimethyl ether.

DME Property	
Carbon content (wt%)	52.2
Boiling point (°C 1 atm)	−24.8
LHV (kJ/mol)	−1328.4
Vapor pressure (20 °C)	5.1
Energy (MJ/L)	20.6

The industrial production of DME is a well-developed technology based on the dehydration of methanol produced from syngas. In the first step, methanol is produced from syngas (Equation (1)), and in a subsequent reactor, the methanol is converted to DME (Equation (2)).

$$CO + 2H_2 \rightarrow CH_3OH \qquad \Delta H^o = -90.6\ kJ/mol \tag{1}$$

$$2CH_3OH \rightarrow CH_3OCH_3 + H_2O \qquad \Delta H^o = -23.5\ kJ/mol \tag{2}$$

where ΔH^o is the standard enthalpy of the reaction.

More recently, the direct synthesis in a one-step process has also been proposed as the most efficient alternative to the two-step process. The one-step process is the combination of the two reactions, methanol synthesis and the methanol dehydration to DME, in the same reactor using hybrid/bifunctional catalysts under conditions close to those of the methanol synthesis reaction. The hybrid/bifunctional catalysts needed for direct DME production requires the combination of metal sites for the selective hydrogenation of CO to methanol, and acid sites for the subsequent methanol dehydration to produce DME. Excellent reviews of catalysts and reactor technologies for the direct synthesis of DME from syngas have been published in recent years [20–27]. The direct synthesis of DME from CO_2, on the other hand, is a much less developed technology, and only a few short reviews of the catalytic systems applied to this technology have been made [21,24–27].

The development of bifunctional/hybrid catalysts for the direct synthesis of DME from CO_2 is challenging because their metal and acid functions needed for the methanol synthesis and dehydration, respectively, must be combined in a correct ratio with controlled interaction. In this context, this paper contains a brief revision of the recent advances in the direct synthesis of DME from CO_2, with special attention paid to the design and strategy that are followed for the development of active and selective heterogeneous catalysts for the direct synthesis. To achieve this objective, this review will analyze the following areas concerning the development of bifunctional/hybrid catalysts for the direct synthesis of DME from CO_2: (i) A comprehensive view of the challenges in thermodynamics and kinetics of the direct hydrogenation of CO_2 to DME; (ii) the analysis of the latest developments in metal and acid functions needed for the methanol synthesis from CO_2 and methanol dehydration; (iii) the revision of the recent strategies for the construction of the bifunctional/hybrid catalysts with emphases on their controlled contact and interaction between metal and acid functions; (iv) the status on catalyst development for direct synthesis of DME from CO_2; and (v) the analysis of the future prospects of making this technology a competitive process will be finally discussed.

2. Direct Synthesis of DME from CO_2: Thermodynamic and Kinetic Considerations

Nowadays, DME is produced at large-scale from syngas (CO + H_2 mixture) by a two-step process via methanol as an intermediate product. In the first reactor, the methanol is produced from syngas over $Cu/ZnO/Al_2O_3$ catalysts (Equation (1)). In a subsequent reactor, the methanol is converted to DME over an acid catalyst (Equation (2)) [13].

$$CO + 2H_2 \rightarrow CH_3OH \qquad \Delta H^o = -90.6\ kJ/mol \tag{3}$$

$$2CH_3OH \rightarrow CH_3OCH_3 + H_2O \qquad \Delta H^o = -23.5\ kJ/mol \tag{4}$$

More recently, the direct synthesis in a one-step process has also been proposed as an attractive alternative to the two-step process [28]. The one-step process is the combination of the two reactions, methanol synthesis (via CO hydrogenation) and the methanol dehydration to DME, in the same reactor using hybrid bifunctional catalysts under conditions that favor the synthesis of methanol. The hybrid catalysts needed for direct DME production require the combination of metal sites for the selective hydrogenation of CO to methanol and acid sites for the subsequent methanol dehydration to produce DME.

The direct synthesis of DME could be more efficient than the two-step process as both reactions are performed in the same reactor, avoiding the intermediate purification and transportation units that allows for lower operating costs [29]. The integration of both reactions in the same reactor also makes the whole process more thermodynamically favorable, leading to the enhancement of both CO conversion and DME selectivity [30]. However, the direct synthesis of DME from syngas is not suitable for commercial purposes, because in the synthesis, the water–gas shift reaction is also simultaneously involved, which means consumption of CO to form CO_2 (Equation (3)). Thus, the net reaction in the direct conversion of CO to DME is represented by Equation (4).

$$CO + H_2O \rightarrow CO_2 + H_2 \qquad \Delta H^o = -41.2\ kJ/mol \tag{5}$$

$$3CO + 3H_2 \rightarrow CH_3OCH_3 + CO_2 \qquad \Delta H^o = -245.8\ kJ/mol \tag{6}$$

The thermodynamic and economic advantages associated with the direct synthesis of DME can be exploited using CO_2 instead of syngas. Compared to the conventional production of DME via syngas (Equation (4)), the formation of DME from the CO_2 requires an extra amount of hydrogen to remove an oxygen atom from CO_2 through the formation of water as a by-product (Equation (5)). In addition, the reverse water–gas shift (RWGS) reaction may occur (Equation (6)):

$$CO_2 + 3H_2 \leftrightarrow CH_3OH + H_2O \qquad \Delta H^o = -49.4\ kJ/mol \tag{7}$$

$$CO_2 + H_2 \leftrightarrow CO + H_2O \qquad \Delta H^o = 41.2\ kJ/mol \tag{8}$$

The thermodynamics for the CO_2-to-DME process is not as favorable as that of the CO-to-DME process, so the yield of DME is lower. The comparative studies of the direct synthesis of methanol and DME from syngas and CO_2 + H_2 made by Ateka et al. [31] indicated that the low DME yield is associated with the lower equilibrium constant of the methanol formation from H_2 + CO_2 feed than for syngas, and its formation is controlled by the participation of the RWGS reaction (Figure 2). Therefore, CO_2 hydrogenation must be carried out near equilibrium to maximize yields of the produced DME.

Direct DME synthesis from CO_2 is favored at high pressure, because of a reduction in the number of moles [32], and at lower temperature because high temperature favors endothermic side reactions such as the reverse water–gas shift reaction that consumes carbon dioxide and hydrogen (Equation (6)). However, the operation at low temperature requires optimization of the reactor designs and innovations such as the in situ water removal (via distillation or membranes) [33] or the development of more active CO_2 hydrogenation catalysts.

A second difference in the direct synthesis of DME from CO_2 with respect to syngas is kinetic in nature and is related to the high production of water associated with the strongly competing reverse water–gas shift reaction that consumes CO_2 and H_2 and reduces the selectivity toward DME. The production of water may also inhibit the production of methanol on the hydrogenation sites of catalysts because water molecules tend to strongly adsorb on the surface of catalysts, blocking the methanol production sites [34]. In addition, water can also affect the acid catalysts responsible for methanol dehydration because water can damage the structure of the acid catalysts.

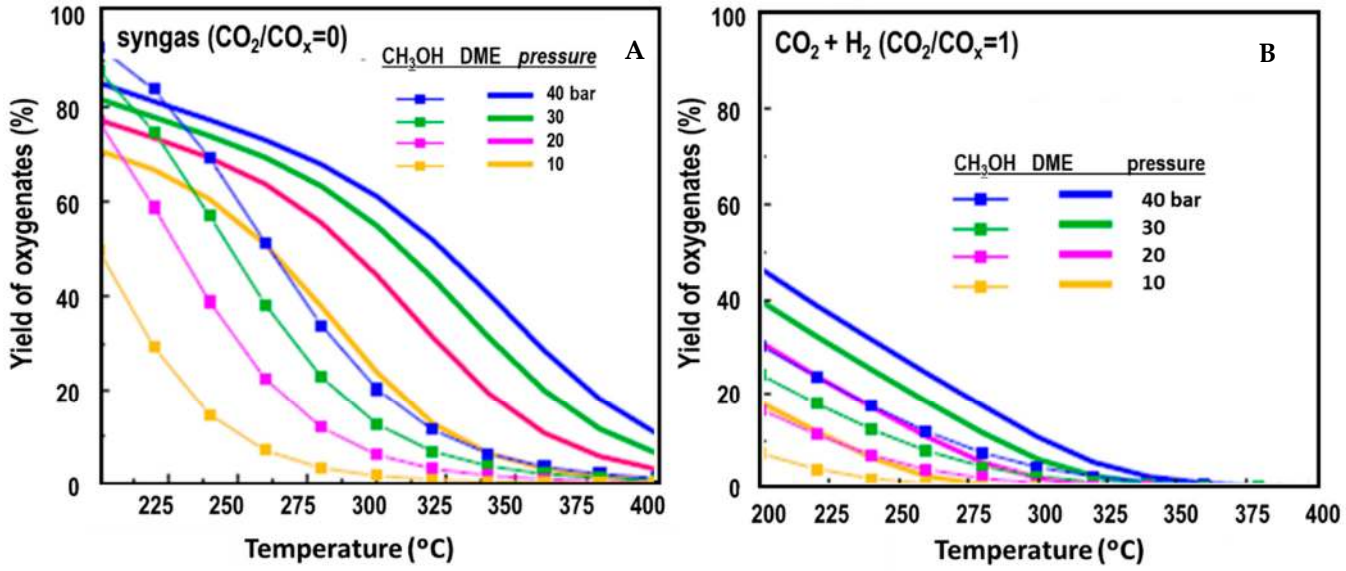

Figure 2. Effects of temperature and pressure on the yield of methanol and dimethyl ether (DME) in the thermodynamic equilibrium of the direct synthesis of methanol and DME from syngas (**A**) and CO_2 (**B**) (adapted from [31] with permission from Elsevier License No. 5015221187364).

3. Catalytic Functions in Bifunctional/Hybrid Catalysts for Direct Synthesis of DME from CO_2

As indicated in the previous section, catalysts for the CO_2-to-DME process require the combination of efficient metal and acids sites for the synthesis of methanol and its subsequent dehydration to DME, respectively (Figure 3).

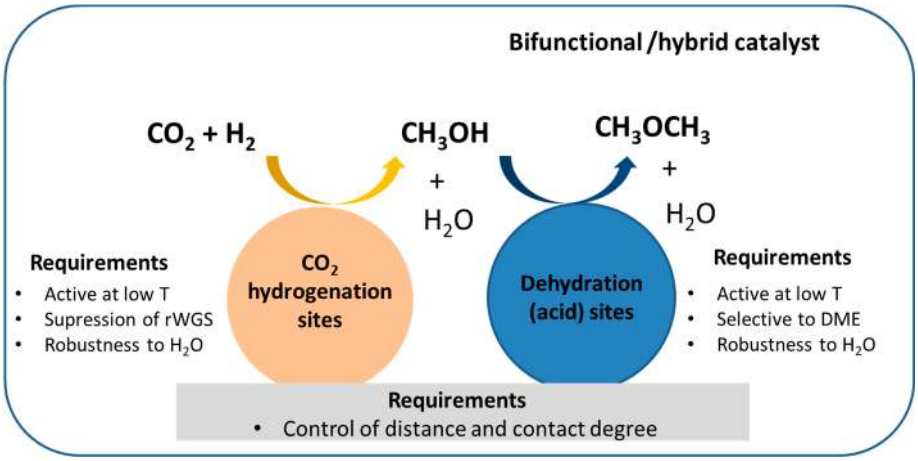

Figure 3. Scheme of bifunctional/hybrid catalysts and requirements for hydrogenation and dehydration functionalities for direct synthesis of DME from CO_2.

The metal and acid functions of the catalysts can be adjusted according to the requirements of the reactions involved (synthesis of methanol from CO_2 and dehydration of methanol), as indicated in the previous section. Therefore, the catalyst function necessary for the hydrogenation of CO_2 to methanol should have a high activity at low temperature to counter the unfavorable thermodynamics of the hydrogenation of CO_2. The hydrogenation function must also minimize the formation of CO during hydrogenation by suppressing the reverse water–gas shift reaction and must be resistant to inhibition and deactivation by water [34,35]. Similarly, acid sites must also be stable in the presence of water, and their number, nature, and strength should also be adjusted to obtain a high dehydration activity at low temperatures compatible with the more thermodynamically favorable conditions

for the methanol synthesis step. However, high acidity should be avoided because it can catalyze secondary dehydration reactions that produce hydrocarbons and carbon deposits. To obtain a good synergy between both functionalities and to avoid their partial deactivation, it is necessary to control the nature and characteristics of the metal and acid sites, their balance, and their distance by maximizing the intimate contact between the metal and acid sites [36].

3.1. Catalytic Function for CO_2 Hydrogenation to Methanol

3.1.1. Conventional Cu-ZnO Catalysts

The first step in the direct synthesis of DME from the mixture of CO_2/H_2 requires the catalytic function for the selective hydrogenation of CO_2 to methanol. Methanol is industrially produced from syngas using conventional Cu/ZnO catalysts [37]. Despite the large number of catalyst formulations explored for the synthesis of methanol from CO_2, the catalysts based on Cu/ZnO systems are most widely used as a starting point for designing catalysts for the direct DME production from CO_2. Recent studies on Cu/ZnO catalysts indicate that CO_2 hydrogenation is related to Cu-Zn synergy in the active sites formed by metallic or partially reduced CuO_x that is in intimate contact with ZnO or partially reduced ZnO_x [38–41]. Despite the complexity of the synthesis of methanol from CO_2, it is known that the Cu-Zn synergistic effect (electronic and structural) depends on the interfacial contact between Cu and ZnO [21,42,43].

In addition to knowledge about the nature of the active sites of Cu-ZnO catalysts, the understanding of the sequence of the elementary steps involved in the hydrogenation of CO_2 to CH_3OH is also a key factor for the improvement in the development of new, more active catalysts for the synthesis of methanol from CO_2. There are two main mechanisms proposed for this reaction: (i) Formate pathway, in which the hydrogenation of CO_2 involves the formation and hydrogenation of reactive intermediate products such as formaldehyde (H_2CO) located on the Zn sites and vacancies [44]; and (ii) the reverse water–gas-shift and CO_2 hydrogenation pathway, where the CO_2 is converted into CO by the RWGS reaction and subsequently hydrogenated to methanol via the formyl and formaldehyde sequence. One of the major mechanistic questions is related to whether methanol synthesis and RWGS are parallel pathways or whether formation proceeds via sequential RWGS and CO hydrogenation. In this respect, recent studies [44] suggest that the formation of methanol from CO_2 does not occur via consecutive RWGS and CO_2+H_2 reactions with the limiting step being the formation of the reactive formiate intermediate on the Zn sites and vacancies (Figure 4) [45,46].

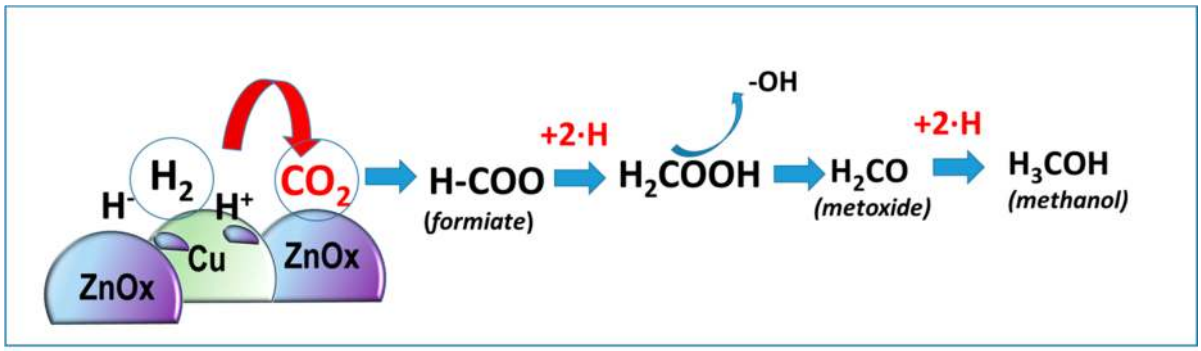

Figure 4. Schematic representation of the elementary steps involved in the hydrogenation of CO_2 to methanol over Cu/ZnO catalysts.

Assuming that the reactions of RWGS and the hydrogenation of CO_2 via formiate follow the parallel mechanism, different active surface sites must be responsible for each reaction in Cu-ZnO catalysts. The independent pathways of RWGS and methanol synthesis pathways on Cu-ZnO catalysts make these catalysts promising candidates for modifications

to increase the methanol yield through the increase in the Zn-promoted Cu active sites for methanol synthesis, minimizing the unpromoted Cu sites active for RWGS.

As indicated above, despite the high activity of Cu-Zn sites for CO_2 hydrogenation, these conventional Cu/ZnO catalysts are not optimal for CO_2 hydrogenation, because they also catalyze the RWGS reaction, an undesired competing reaction that reduces conversion and selectivity toward methanol in the direct hydrogenation of CO_2. The inhibition of the Cu/ZnO catalyst by water is due to its strong adsorption on active Cu-Zn sites which promotes the oxidation and growth of the Cu and ZnO particles, leading to the lowering of the activity of the Cu/ZnO catalysts in the low-temperature reaction [35]. Both factors limit the application of the Cu/ZnO catalysts for CO_2 hydrogenation to methanol. To enhance the catalyst effectivity of Cu/ZnO catalysts for methanol synthesis from CO_2, an increment in the concentration of the highly active Cu-Zn sites is required at the expense of the unpromoted Cu sites catalyzing the RWGS reaction [46]. For the optimization of Cu/ZnO catalysts, three main strategies are developed (Figure 5): (i) An increase in Cu dispersion through new synthesis strategies [47]; (ii) optimized promotion through the addition of modifiers; and (iii) the design of the new class of non-Cu-based catalysts. Some of the most important developments that followed the last two strategies are summarized in the following sections.

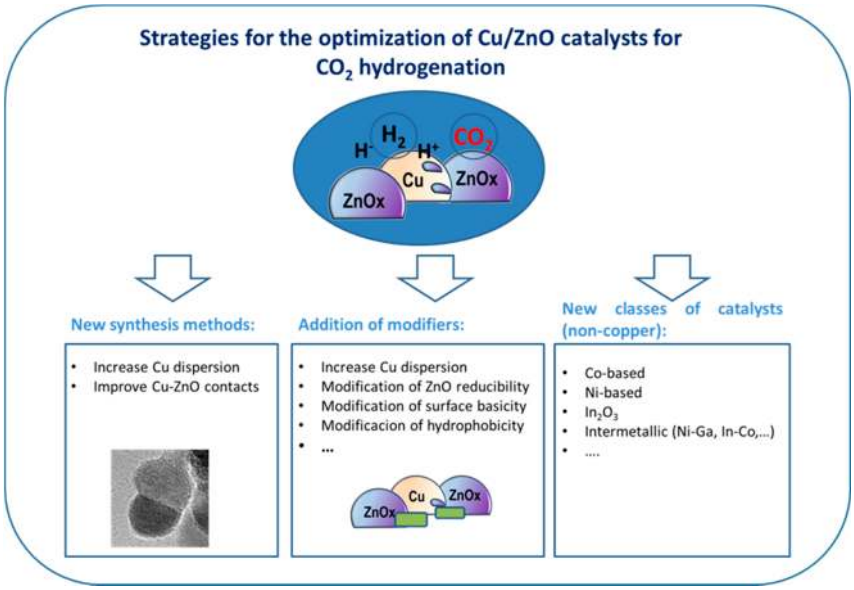

Figure 5. Main strategies followed for the optimization of Cu/ZnO catalysts applied for methanol synthesis from CO_2 hydrogenation.

3.1.2. Modified Cu-ZnO Catalysts

Recently, many attempts were made to modify the conventional Cu-ZnO catalysts to enhance the CO_2 conversion and the selectivity toward methanol. As stated above, the production of methanol from CO_2 hydrogenation is closely related to the formation of Cu-ZnO contacts for methanol synthesis, decreasing the nonpromoted Cu sites active for r-WGS. In this sense, several attempts have been made to enhance the activity of Cu-ZnO catalysts by the addition of different modifiers to change the Cu dispersion, reducibility, surface basicity, hydrophobicity, etc.

Cu-ZnO catalysts are usually promoted with Al_2O_3 that act as a structural promoter, improving the stability and thermal resistance [48]. In addition, the electronic modification of the ZnO lattice by Al^{3+} ions favor the reduction of ZnO, which in turn, favors the formation of active Cu-ZnO sites [49]. In a similar strategy, different modifiers such as Ga^{3+} [50], Cr^{3+}, and Mn^{2+} [51] have been studied as promoters of Cu-ZnO catalysts for their use for direct DME production from CO_2. For example, the promoter effect of Ga^{3+} was associated with its insertion into the ZnO lattice that facilitates the reducibility of

ZnO, which facilitates the Cu-Zn synergy in active sites formed by metallic Cu promoted by an intimate contact with reduced ZnO_x [52,53]. The enhancement of the reducibility of ZnO by Ga^{3+} ions is related to the electronic heterojunction between $ZnGa_2O_4$ and ZnO that also facilitates the adsorption of intermediates (HCO, H_2CO, and H_3CO) and their transformation into methanol. In the case of the promotion of Cu-ZnO by Mn^{2+}, the improvement of the conversion of CO_2 was linked to the improvement of the dispersion of Cu, favoring the contact of Cu with ZnO species, as well as to the decrease in the CuO reduction temperature, leading to an increase in the specific surface and stability of the Cu-ZnO active sites [54–56].

Another method to improve the activity of Cu-ZnO catalysts in the synthesis of methanol from CO_2 was by forming an alloy between Cu and noble metals (Pt, Rh, Pd) [57–60]. In general, the addition of small amounts of noble metals to Cu-ZnO resulted in the higher development of Cu-ZnO active sites and a marked improvement in the adsorption of H^+/H^- and CO_2 on the catalysts surface that increased the rate of methanol production from CO_2 hydrogenation reaction. Despite improvements in the activity/selectivity of Cu/ZnO catalysts after the incorporation of noble metals, this alternative has limited practical use due to the high price associated with the use of noble metals.

One of the most studied modifiers for the improvement of the Cu-ZnO catalyst is ZrO_2 [61–66]. In this sense, the Cu-ZnO–ZrO_2 catalytic system is considered more effective than the traditional Cu–ZnO–Al_2O_3 catalyst, showing relatively high CO_2 conversion (23%) and high methanol productivity (331 g_{CH3OH} $kg_{cat}{}^{-1}$ h^{-1}) at mild reaction conditions (280 °C, 50 bar, and gas hourly space velocity (GHSV) of 10,000 h^{-1}) [64]. The enhanced behavior of the Cu-ZnO-ZrO_2 system is related to both the weak hydrophilic character of zirconium oxide that hinders the strong adsorption of water and the increase in the surface basicity, which facilitates the CO_2 adsorption and, therefore, the methanol productivity. It was hypothesized that ZrO_2 could also have the ability to activate the adsorbed CO_2, favoring the formation of CO_2* species. These CO_2* species could then react with the H_2* species to form intermediate species (i.e., formate/dioxomethylene/methoxy) during the time course of methanol synthesis [64]. In addition to that, ZrO_2 favors the formation of oxygen vacancies during reduction that facilitates the Cu dispersion and increases the Cu-ZnO contacts. The increase in the stability of the $Cu^{\delta+}$ sites by interaction with zirconia explains both the improvement in Cu dispersion and the increase in the Cu-ZnO contacts [65].

Mesoporous silica and carbonaceous materials have also been reported as less conventional promoters of Cu-ZnO catalysts for CO_2 hydrogenation to methanol [27,67,68]. The combination of Cu-ZnO with SBA-15 allows for the confinement of the Cu-ZnO active sites within the mesoporous structure of SBA-15, which improves the inter-particle spacing, distribution, and stability of Cu-ZnO sites with respect to unpromoted Cu-ZnO [67]. The confinement in the mesoporous structure also improves the contact of the Cu-Zn active sites with H_2 and CO_2, resulting in better activity and selectivity to methanol production (376 $mg_{(CH3OH)}$ h^{-1} $g_{cat}{}^{-1}$, 50 bar, 280 °C, GHSV = 6000 h^{-1}) compared with the conventional Cu-ZnO catalyst. Carbon nanotubes, graphene oxides, or coordination polymers are also studied as carbonaceous modifiers to enhance the activity of Cu-ZnO catalysts in the methanol synthesis from CO_2 [69–71]. The use of carbon nanotubes reduces the dimensions of the Cu-ZnO nanoparticles, facilitating its surface exposition and reducibility that allows for the increase in its activity and stability during the hydrogenation of CO_2 to methanol [70]. A similar improvement was reported for Cu-ZnO particles when highly dispersed on reduced graphene oxide aerogel (2950.4 μmol_{CH3OH} $g_{cat}{}^{-1}$ h^{-1} at 250 °C and 1.5 MPa) [71]. Carbonaceous coordination polymers combined with Cu-ZnO catalysts is also a strategy that is followed to obtain evenly distributed Cu-ZnO nanoparticles that generate a high number of Cu–ZnO interfacial sites stabilized by the coordination polymers. This makes it possible to inhibit the strong adsorption and deactivation of the active sites of Cu-ZnO by water while maintaining the catalyst activity and the selectivity to methanol [70].

TiO_2 has also been explored as a promoter of the Cu-ZnO catalysts for CO_2 hydrogenation to produce methanol according to the results of Xiao et al. [71]. The use of TiO_2 allows for the formation of oxygen vacancy sites for CO_2 activation and interaction with the Cu-ZnO active sites. The catalytic activity exhibited a volcano curve trend with increasing TiO_2 content. The methanol yield increased linearly with the TiO_2 loading due to the improved adsorption of CO_2 on the surface of catalysts and its reaction on the active sites of Cu-ZnO. The addition of TiO_2 affected CO_2 adsorption only without modifying the intrinsic activity of the Cu-ZnO sites [71].

3.1.3. Alternative Non-Copper Catalysts

As stated above in addition to the low activity, the Cu-ZnO catalysts also show poor stability during the hydrogenation of CO_2 due to Cu sintering and the mobility of ZnO accelerated by the generated water [35]. Therefore, non-Cu-based catalysts are being studied as alternative systems to Cu-ZnO catalysts. As compared with Cu-based catalysts, the studies on methanol synthesis from CO_2 over non-copper-based systems are scarce. In general, most of the non-copper catalysts are based on noble metals, mainly Pd/ZnO [72], Pd/In_2O_3 [73], and Au/ZrO_2 [74]. However, from a practical point of view, the most interesting are those that do not have noble metals in the formulation as they can compete in cost with the conventional Cu-based catalysts. Therefore, we will focus in this section only on catalysts based on nonnoble metals (Co, Ni, In-Ni, In-Ga, In-Co, etc.). Readers interested in noble metal-based catalysts applied to CO_2 hydrogenation may consult some excellent reviews recently published in the area [44,75].

Nonnoble catalysts based on cobalt show promising performance for methanol synthesis from CO_2 hydrogenation [76,77]. The high performance of those catalysts was attributed to the CoO phase, which improves the selectivity to CH_3OH by inhibition of the reverse water–gas shift reaction. Despite the interesting results obtained on the Co-based catalysts, the mechanism of the active sites operating on these Co-based catalysts (inhibiting RWGS) is not yet determined and needs to be clarified. Ni-based catalysts were also proposed as effective nonnoble methanol synthesis catalysts for the hydrogenation of CO_2 [77]. Interesting activity results were reported for Ni particles supported on β-Ga_2O_3 tested at 0.5 MPa [78]. Small Ni NPs with an average size of about 3.3 nm exhibited the best catalytic response, which was associated with their large perimeter contact with the Ga_2O_3 support. However, an enhanced selectivity toward methanol formation was achieved on the catalysts with the largest Ni nanoparticles (10.2 nm) deposited on the β-Ga_2O_3 support. The smaller nanoparticles of Ni promote the rWGS reaction, while the larger ones in contact with gallium oxide facilitate the stabilization and hydrogenation of intermediate species (formate/dioxomethylene) during the time course of methanol synthesis.

In recent years, In_2O_3 has received considerable attention as a catalyst for the synthesis of methanol from CO_2 due to their excellent behavior in the temperature range between 200 and 320 °C [79]. At a low CO_2 conversion of 5.5% (300 °C, 5.0 MPa, 20,000 $mL g^{-1} h^{-1}$), the In_2O_3 cubic phase exhibited almost a 100% selectivity to methanol [80]. Defective oxygen vacancies on In_2O_3 are considered the active sites for CO_2 activation and stabilization of the HCOO, H_2COO, and H_2CO intermediates. The high selectivity of In_2O_3 to methanol was also suggested to be related to the fact that In_2O_3 might inhibit the rWGS reaction [80]. The activity and stability of In_2O_3 improve when it is combined with ZrO_2 [81]. It was suggested that the better activity of the In_2O_3/ZrO_2 catalysts was related with the interaction between both components that change the reaction pathway [81]. The formation of surface oxygen vacancies on In_2O_3 was reported to be beneficial for the selective synthesis of CH_3OH [82]. In_2O_3 modified with Ga was another catalytic system efficient for the selective hydrogenation of CO_2 to methanol at high temperature (300–400 °C) [83]. The insertion of Ga into the In_2O_3 lattice promotes the generation of surface oxygen vacancies in In_2O_3 that produces changes in the surface adsorption of the key intermediates (HCOO, H_2COO, and H_2CO), promoting by this way the selective formation of methanol. The con-

centration of surface oxygen vacancies in In_2O_3 is controlled by the Ga/In ratio, achieving the maximum methanol yield for the Ga/In ratio of 0.4/1.6 [83].

Various non-noble intermetallic compounds (Ni-Ga [84], In-Co [85], and In-Ni [86] have also been studied as new formulations for the synthesis of methanol from CO_2. Among these, Ni-Ga intermetallic catalysts (Ni_5Ga_3) supported on SiO_2 were reported as more active and selective for the hydrogenation of CO_2 at ambient pressure than conventional $Cu/ZnO/Al_2O_3$ catalysts [84]. Selective methanol production in these intermetallic catalysts was associated with Ni-Ga sites that promoted CO_2 activation. Other interesting intermetallic catalysts are those based on Ni-In supported on SiO_2 [86]. In these systems, small Ni-In-Al intermetallic particles were prepared from phyllosilicate precursors with an Ni/In ratio between 0.4 and 0.7. Catalysts showed a higher activity and selectivity toward methanol compared to those obtained on the conventional $Cu/ZnO/Al_2O_3$ catalyst (0.33 against 0.17 mole CH_3OH $(mole_{metal\ catalyst})^{-1}$ h^{-1}) [86].

3.2. Catalytic Function for the Dehydration of Methanol

Generally, it is accepted that the dehydration of methanol to DME ($2CH_3OH \leftrightarrow CH_3OCH_3 + H_2O$) might occur either on Brønsted acid sites or Lewis acid–base sites. However, the observed increase in the reaction rate with the increase in the surface Lewis acid sites strongly suggest that this reaction mainly occurs on Lewis acid sites [87,88], although the involvement of the Brønsted acid sites is also important. In general, the most active catalysts are those that possess stronger acid sites; however, the strength of Brønsted sites must be controlled in order to prevent the formation of undesired hydrocarbons [87,88]. The catalysts used for the methanol dehydration to DME are based on acid solids such as crystalline alumina-silicates, γ-Al_2O_3 [87–89], the H-form of zeolites, sulfated zirconia, and clays [13,27]. Among the great variety of solid acid catalysts, recently reviewed by Bateni and Able [90], the most commonly used are the H-form of zeolites and γ-Al_2O_3 because of their optimal acid strength (weak- and medium-strength acid sites) needed for the methanol dehydration.

In general, the mechanism for methanol dehydration can be described as the reaction between two molecules of methanol adsorbed on acid sites that, depending on the temperature and methanol pressure, can follow two different routes: (i) Associative or (ii) methoxy-mediated dissociative route, which needs Brønsted acid sites [91]. A schematic illustration of both routes during the methanol dehydration is shown in Figure 6. In the dissociative mechanism, methanol adsorbs on acid sites, losing a water molecule and transforming into a surface methoxy group. Subsequently, nucleophilic attack on the surface methoxy by a second methanol molecule leads to the formation of DME. By contrast, in the associative mechanism, DME and water molecules are formed from two methanol molecules co-adsorbed at acid sites [91].

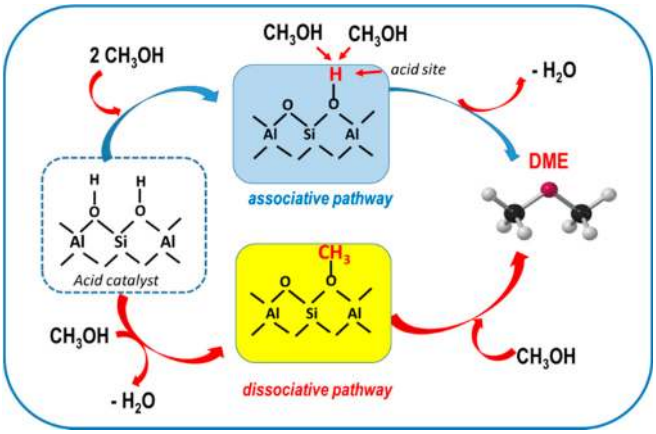

Figure 6. Scheme showing the associative and dissociative routes of the methanol dehydration on acid sites.

Regardless of the nature of the acid sites, the dissociative mechanism must be dominant under specific reaction conditions employed, as was recently demonstrated in a DFT study conducted by Ghorbanpour et al. [91]. However, at higher temperatures where entropic contributions are high, the mechanism changes from associative to dissociative due to the change in temperature requirements for each active site. At high methanol partial pressure, the adsorbed methanol becomes stabilized through dimer formation, which undergoes subsequent dehydration to DME. At such conditions, dissociation of the H-bonded methanol became less favorable due to the enhancement of dimers formation [92]. In the case of the H-form of zeolites, both pathways, associative or dissociative, are catalyzed by Brønsted acid sites. In the reaction mechanism based on the Lewis acidity, the reaction between the adsorbed methanol molecule on an acidic site and an adsorbed alkoxide anion on a basic site is assumed. In such a case, the presence of adjacent acid–base pair sites on the catalyst surface is needed [93].

3.2.1. Al_2O_3-Based Catalysts

As indicated in the previous section, Al_2O_3-based materials (γ-Al_2O_3 [87] and η-Al_2O_3 [88]) are considered the benchmark catalysts for the dehydration of methanol to DME. This is because both substrates are typical Lewis acid catalysts with mainly weak- and medium-strength acid sites. In addition, the alumina-based catalysts are interesting for the DME production because of their low cost and interesting properties such as high surface area, mechanical strength, and excellent thermal stability. The reaction mechanism on γ-Al_2O_3 is based on the interaction between the methanol molecule adsorbed on an acidic Lewis site (Figure 7) with an alkoxide anion adsorbed on an adjacent basic site [93]. The reaction mechanism in the case of η-Al_2O_3, investigated recently by Osman and Abu-Dahrieh [94], undergoes a Langmuir–Hinshelwood mechanism in which the methanol molecules adsorb dissociatively on the Lewis acid sites of the surface.

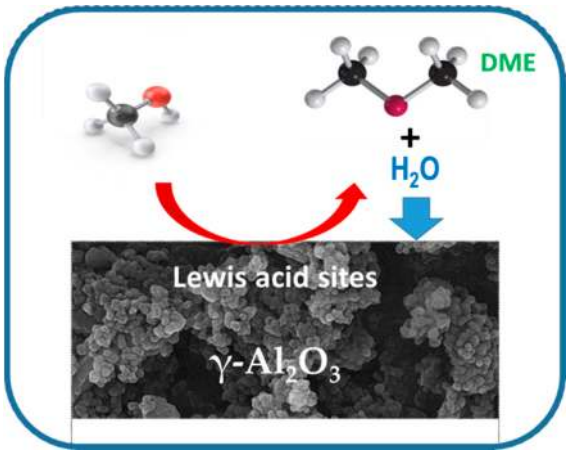

Figure 7. Schematic illustration of the methanol dehydration to DME on Lewis acid sites of γ-Al_2O_3.

The main drawback for the application of Al_2O_3-based acid catalysts in the direct CO_2 conversion to DME is the need for a high reaction temperature (>300 °C not compatible with the temperature for CO_2 hydrogenation of 250–300 °C) and the loss of activity due to the adsorption of water, which implies the need to develop alternative formulations [95]. To avoid Al_2O_3 deactivation by water adsorption, it is necessary to modify its superhydrophilic properties. Among various factors influencing the hydrophilic behavior of γ-Al_2O_3, those linked with their synthesis conditions are most decisive. Therefore, to modify the hydrophilic behavior and to enhance the specific surface area of Al_2O_3-based acid catalysts, different synthesis [96] and structure modification methods [97] have been explored. The influence of synthesis conditions on the activity and physico-chemical properties of γ-Al_2O_3 catalysts was studied by Yaripour et al. [98]. Using the fractional factorial design, the authors optimized the conditions of catalyst preparation by precipitation. The

activity results in the dehydration of methanol indicated that the behavior of γ-Al_2O_3 is mainly influenced by the pH of the precipitation solution, type of precipitant, and mixing rate. The best results were obtained with the optimized catalyst possessing the pure γ-alumina crystallite phase and high specific surface area (251.5 m^2 g^{-1}) that achieves high methanol conversion (78.2%) [98]. Recently, the study by Carvalho et al. [97] showed that the Cu-ZnO supported on alumina modified by Si exhibited high performance in the direct hydrogenation of CO_2 to DME (T = 270–290 °C, P = 30–50 bar). The improvement in activity was associated with changes in the acid strength of the alumina derived from the Si insertion into the Al_2O_3 structure [97].

The modification of the amount of weak Lewis acid sites in Al_2O_3-based catalysts was also studied by its modification with Group 11 elements, such as Ag, Au, and Cu, which act as electron acceptors. The modification of η-Al_2O_3 with different Ag loadings (1%, 10%, 15% *w/w*) and its effect on the production of DME via methanol dehydration were investigated by Osman et al. [88]. The Ag/η-Al_2O_3 catalysts were evaluated in a fixed-bed reactor at a temperature range of 180–300 °C and WHSV of 48.4 h^{-1}. It was found that the catalyst activity was improved with the Ag loading of 10% *w*/*w* as the optimum silver loading. The enhancement of the catalyst activity was linked with an improvement in the Lewis acidity and of the bulk surface properties by changing the surface from superhydrophilic to hydrophilic [88]. Similarly to Ag/η-Al_2O_3 catalysts, the alumina modification with Cu was found to be beneficial for the methanol dehydration reaction, as it was demonstrated by Chiang et al. [99]. The catalytic response of Cu-Al_2O_3 catalysts was evaluated in the methanol-to-DME reaction in a temperature range of 150–350 °C and 50 bar. It was found that the nature of the copper entities had a marked impact on the product distribution. Interestingly, under the conditions they used, the formation of $CuAl_2O_4$ spinel mixed oxide occurred. According to Chiang et al. [99], methanol dehydration might occur on the $CuAl_2O_4$ sites, whereas CuO and metallic Cu species could be responsible for the decomposition of methanol and the production of both methanol and formic acid, respectively.

The formation of DME via catalytic dehydration of methanol was also achieved by the promotion of Cu/γ-Al_2O_3 catalyst with hematite (Fe_2O_3), as it was demonstrated by Olivas and co-workers [100,101]. The possible reaction mechanism proposed by authors is shown in Figure 8. Upon the reaction conditions employed (290 °C and atmospheric pressure), the methanol conversion over the Cu-Fe_2O_3/γ-Al_2O_3 catalyst was found to be 70%, which is similar to other catalytic systems tested in harsh conditions. Noticeably, this bimetallic catalyst exhibited a 100% selectivity toward the DME production. The spent catalyst exhibited an absence of changes in the chemical oxidation states of Cu and Fe after the reaction confirmed by XPS. The methanol conversion was maintained after catalyst regeneration at 600 °C for 2 h in air, showing the reusability of the Cu-Fe_2O_3/γ-Al_2O_3 catalyst [101].

3.2.2. Zeolite-Based Catalysts

Zeolites are porous aluminosilicates with a high specific surface area and a regular crystalline framework structure comprising silicates (SiO_4) and aluminates (ions) linked in tetrahedral positions via oxygen atoms. Both natural and synthetic zeolites have great potential for producing DME from methanol at suitable reaction conditions. However, their activity, selectivity, and stability strongly depend on their physicochemical properties. Noticeably, zeolites exhibit a better tolerance to the adsorption of water in comparison to Al_2O_3-based catalysts and, in consequence, they showed better catalytic activity [102]. However, zeolites possess various inherent strong acid sites that usually create unexpected products, which might cause the formation of coke deposits. The product distribution in methanol dehydration is strongly affected by the zeolite morphology (shape and dimensions of the internal channels and cages) and acidity [102,103], whereas their hydrophilic/hydrophobic behavior is known to be affected by the SiO_2/Al_2O_3 ratio [104].

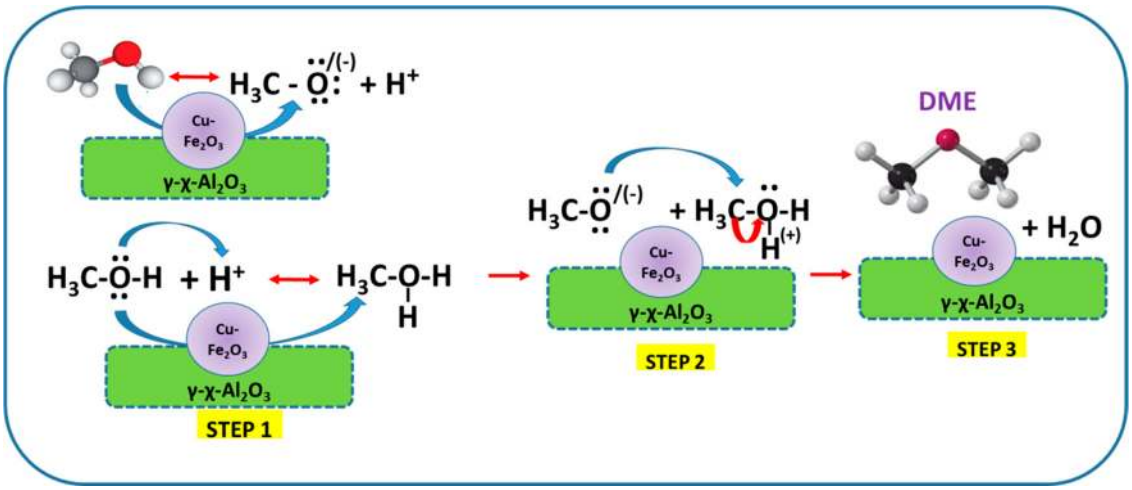

Figure 8. The possible reaction mechanism of methanol dehydration to DME over Cu-Fe_2O_3/γ-Al_2O_3 catalyst (adopted from [102] with permission from Elsevier License No 5015231376777).

The comparison of the catalytic behavior of BEA, MFI, and FER zeolites with the same Si/Al ratio and different pore sizes and topology clearly demonstrated the best results over the largest-pore 3-D framework zeolite (BEA) [102,103]. However, this zeolite exhibited deactivation at short times on stream due to the fast coke formation favored by the large channel size and topological connection spaces. In comparison with BEA, a lower coke formation was observed for MFI zeolite with medium pores and a 3D framework structure. As compared with BEA and MFI zeolites, the small 2-D pores of FER zeolite showed the best stability and a good selectivity toward DME at high temperature [102,103]. Other zeolites (ZSM-5, ferrierite, HY, clinoptilolite, and mordenite) were also deeply investigated for use in the dehydration of methanol to DME and usually used in the H-form (H-ZSM-5, H-Y, and H-mordenite). Despite the large number of zeolites explored for the dehydration of methanol to produce DME, those based on ZSM-5 and FER structures are most commonly used because of their suitable texture and acidity.

The H-ZSM-5 is the most studied zeolite as an acid catalyst for methanol dehydration. This is mainly because of its large amount of Brønsted acid sites and its hydrophobic characteristic, making this zeolite more resistant toward the poisoning of acid sites by water (Figure 9). There is a controversial discussion between the use of γ-Al_2O_3 and H-ZSM-5 for DME synthesis, as HZSM-5 presents stronger acidic sites, which lead to the formation of undesired light hydrocarbons as by-products, and the catalyst deactivation by coke formation [105]. The smaller crystallite size of H-ZSM-5 zeolite and the lower concentration of Brønsted acid sites on the zeolite external surface with respect to those of alumina could be beneficial for the activity [106]. However, the optimization of Si/Al ratio in HZSM-5 zeolites is essential to adjust its acidity before its application as acid catalysts for the dehydration of methanol with high activity and good stability against water deactivation. The effect of the Si/Al ratio of HZSM-5 zeolites on its activity and selectivity to DME by dehydration of methanol has been studied in the literature [107]. An enhancement of the catalyst activity was observed with the increase in the aluminum content explained by the increase in the amount of strong acid sites.

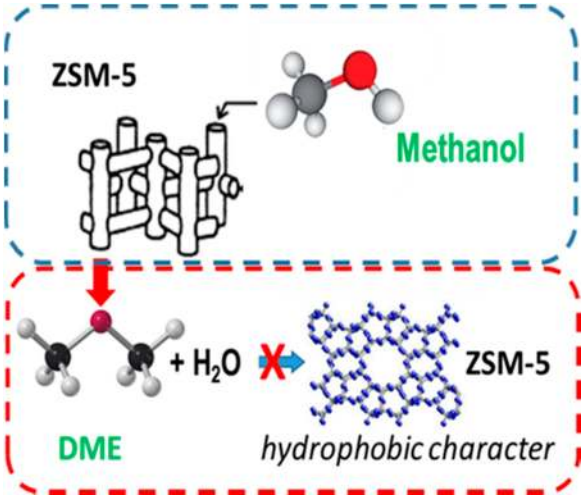

Figure 9. Schematic illustration of the methanol dehydration to DME on hydrophobic ZSM-5 zeolite.

The chlorination and fluorination of zeolites were demonstrated to be effective methods to tune the catalytic acidity [108,109]. The effects of the zeolite halogenation and ultrasonication of HZSM-5 zeolites on their physicochemical properties and catalytic behavior in the dehydration of methanol were investigated by Aboul-Fotouh et al. [109]. The chlorinated and fluorinated HZSM-5 zeolites showed enhanced catalytic activity with the chlorinated zeolite catalysts being more active and selective toward DME production than their respective fluorinated versions. An additional enhancement in the catalytic activity for DME formation was achieved over chlorinated ZSM-5 zeolites prepared by ultrasonic irradiation. This enhancement was explained as due to positive changes in the textural and acidic properties occurring upon ultrasonic irradiation [109]. Similar effects were described for the sonicated and fluorinated H-MOR zeolites. Another way to control the acidity of HZSM-5 is related with its desilication. Aloise et al. [110] observed an improvement in the methanol dehydration activity and stability associated with the desilication of the ZSM-5 zeolite. The improved catalytic performance was related to modifications in the acidic and textural properties of the ZSM-5. The increase in the Brønsted acid sites and average mesopore diameter with desilication allow the formation of a larger amount of accessible active sites, which favored the DME production and minimization of the formation of coke deposits [110]. The selectivity toward DME of ZSM-5 catalysts could also be enhanced by adding low amounts of methyl mono- and dicarboxylate esters as additives, as it was recently demonstrated by Dennis-Smither et al. [111]. The process was easily reversible and the DME yield depended on the additive concentration [111].

The study by Magzoub et al. [112] demonstrated that the use of the H-ZSM-5-structured catalyst in the form of the monolith considerably enhanced the selectivity to DME with respect to H-ZSM-5 powder. The achieved DME selectivity was 96% with a methanol conversion close to 70% at 180 °C. Monolithic conformation produced alterations in the acidity and porosity properties. The zeolite monolith exhibited a slight reduction in the number of the strong and Brønsted acid sites, and a higher micro/mesoporosity that facilitates the methanol and DME diffusion [112].

The dehydration of methanol was also studied over other zeolite types as the H-form of FER-type and MFI-type zeolites [113]. To obtain evidence of the influence of acidity, both zeolites were prepared with different Si/Al ratios. It was found that both the zeolite structure and Si/Al ratio strongly affected the methanol dehydration reaction, with the Si/Al ratio of 10 as the most optimized one. The FER-type zeolite showed higher activity and selectivity for the dehydration of methanol to DME than the FER-type counterpart. The water tolerance of FER-type zeolites in the methanol dehydration to DME was investigated by Catizzone et al. [113]. FER-type zeolites were synthesized with different Si/Al ratios to obtain catalysts with different acidic functions. FER-type zeolites with a crystal size in the

range of nanometers exhibited enhanced accessibility to the acid site. As a consequence, ferrierites showed a higher mass transfer capacity than γ-Al_2O_3 in reaction at temperatures below 200 °C. In another study by the same authors, the larger ability of the Lewis acid sites of FER and MFI zeolites than Brønsted acid sites was confirmed for the methanol dehydration to DME. The highest DME yield was achieved at 180 °C with FER zeolite (Si/Al = 10) possessing Lewis acid sites and higher acidity [113]. However, zeolites showed a decrease in the selectivity to DME at temperatures above 200 °C, and this decrease is more pronounced as acidity and temperature increase. The incorporation of water into the feed caused an insignificant decrease in the conversion of methanol over ferrierites, as opposed to γ-Al_2O_3, which showed a notable inhibition. In addition, FER zeolites showed a lower tendency to form coke when the water was co-fed with methanol [113].

H-Mordenite and H-Beta zeolites were also acid catalysts studied for the dehydration of methanol. For example, the effects of the physical and chemical treatments of H-Mordenite and H-Beta zeolites on their efficiency in the reaction of methanol dehydration to DME were investigated by Solyman et al. [114]. The physical modification of both zeolites was performed via ultrasonication, whereas their chemical modification was made by impregnation with aluminum nitrate. The characterization of modified zeolites demonstrated that the physical modification of H-Mordenite and H-Beta by ultrasonication led to a two-step transformation into small crystals followed by a compaction process. In the case of the chemical treatment, both zeolites exhibited alumina species decorating the surface of zeolite and located within their inner structure. From the catalyst acidity–activity correlation, the enhancement of the catalyst efficiency toward DME over modified H-Mordenite and H-Beta was concluded to be due to the formation of medium- and strong-strength acid sites on the catalyst surface. Regardless of the catalyst modification method and the reaction contact time, the methanol conversion and DME selectivity over all catalysts were found to be 100% at 200 and 225 °C, respectively.

3.2.3. Heteropolyacids (HPAs)-Based Catalysts

To avoid the disadvantages of the use of zeolites in the reaction of the dehydration of methanol, a promising alternative could be the use of heteropolyacids (HPAs) immobilized on high surface supports. Heteropolyacids are widely used in acid catalytic reactions due to their exceptionally strong Brønsted acidity, thermal stability, and ability to operate under milder conditions than those required by alumina or zeolite. Heteropolyacids have different structures and their general formula is $H_nXM_{12}O_{40}$, in which n is the number of acidic protons, X is a heteroatom (often P^V, Si^{IV}), and M is a transition metal (typically Mo^{VI}, W^{VI}). The most acidic HPAs, namely $H_3PW_{12}O_{40}$ and $H_4SiW_{12}O_{40}$, studied for the CH_3OH-to-DME reaction exhibit Keggin's three structured levels (Figure 10): (i) The primary structure is of the heteropolyanion itself; (ii) the secondary structure consists of a three-dimensional organization with H^+ and H_2O; and (iii) the tertiary structure possesses the arrangement of particles responsible for the surface of HPA [115]. Both the structuration level of HPA (primary, secondary, and tertiary) and its water content determine the location, number, and strength of its acid sites [115]. The flexibility of the HPA structures to absorb polar molecules such as methanol and dehydrate it in its bulk structure (pseudo-liquid behavior) could enhance the dehydration capacity of HPAs because it could dehydrate at surface and bulk levels. Thus, the water content in HPA is one of the main factors influencing the activity of HPAs, as it determines the strength and accessibility of its acid sites to react with methanol [116].

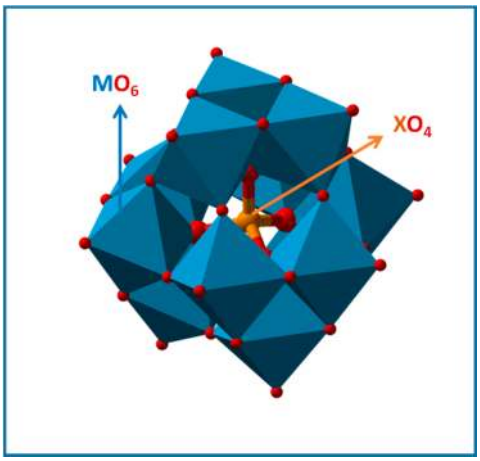

Figure 10. Keggin structure of heteropolyacids.

The HPAs show a low surface area (around 5–10 m^2/g) and is therefore helpful for supporting the HPAs on different substrates (TiO_2, SiO_2, ZrO_2, carbon nanotubes, boron nitrides, etc.) as a strategy to enhance the activity of HPAs in the methanol dehydration reaction [117–120]. In particular, silicotungstic acid ($H_4SiW_{12}O_{40}$, HSiW) supported on TiO_2, SiO_2, and ZrO_2 showed a high activity in this reaction, being more active than bulk HSiW [121]. This enhancement of catalytic activity was associated with the improvement in the accessibility of the methanol to the acid sites due to an improvement in the interchange between methanol and crystallization water. Operation at temperatures above 180 °C limits the access of the methanol to the bulk structure and, therefore, means the loss of the pseudo-liquid behavior of HPAs [121]. TiO_2-supported heteropoly acids (HPAs) also exhibited very high catalytic activities for the dehydration of methanol [118]. For both TiO_2-supported HPW and HSiW, it was found that the production of DME per acid site increases with the HPAs loading, reaching a maximum for the catalyst containing 2.3 HPA units·nm^{-2} (Figure 11). At this optimum loading, both HPW and HSiW were well dispersed onto the support surface, permitting the easy access of methanol to the active acid sites. The effect of supporting tungstophosphoric acid ($H_3PW_{12}O_{40}$, HPW) on TiO_2 on the activity of a hybrid catalyst containing Cu-ZnO(Al) and HPW/TiO_2 as metal and acid functions, respectively, was investigated recently in the direct CO_2 hydrogenation to DME [122]. In good agreement with the study by Ladera et al. [123], it was found that the amount of HPW employed for TiO_2 modification should be optimized. The best catalytic result was achieved with the catalyst having TiO_2 decorated with 2.7 monolayers of heteropolyacid. Noticeably, the activities of this catalyst was higher than that of the reference hybrid Cu-ZnO(Al)/HZSM-5 catalyst, typically employed for DME production. However, the catalyst modified with an optimized amount of HPW exhibited some kind of catalyst deactivation under the reaction conditions employed [122].

The study by Kornas et al. [124] examined the effect of the type of HPA ($H_3PW_{12}O_{40}$ (HPW) and $H_3PMo_{12}O_{40}$ (HPMo) supported on montmorillonite K10 on the activity of the hybrid catalyst combined with CuO/ZrO_2 in the direct CO_2 hydrogenation to DME. Due to the higher acidity of HPW compared to HPMo, the HPW-modified catalyst proved to be more active and stable under the reaction conditions employed than its HPMo-modified counterpart. The acidity of the catalyst and its thermal stability were the main factors influencing the catalytic activity [124].

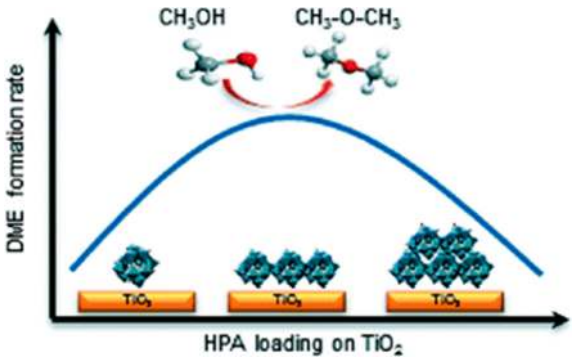

Figure 11. Influence of heteropoly acids (HPAs) loading on TiO_2 on the DME formation rate (adapted from [118] with permission from RSC License No 1099726).

Phosphotungstic and silicotungstic acid salts (CuPW, CuSiW, FePW, FeSiW) were also studied in the reaction of dehydration of methanol [125]. Copper salt catalysts showed a high DME selectivity (100%) at low temperature (100–250 °C), while the FeSiW and FePW salts showed similar DME selectivity at higher temperature (250 °C). The silicotungstic acid salts were most stable under the reaction conditions (120 h lifetime) than the phosphotungstic counterparts.

3.2.4. Other Acid Catalysts

Alternative acid catalysts based on silicoaluminophosphates (SAPO, such as SAPO-11, SAPO-34, and SAPO-18) are also the subject of study for application in the DME synthesis via methanol dehydration. SAPO-11 is of particular interest because it is a medium-pore silicoaluminophosphate molecular sieve with a structure of regularly alternating tetrahedral AlO_4, PO_4, and SiO_4. Its one-dimensional channel topology with an elliptical pore aperture of 0.4 nm x 0.6 nm minimizes the retention of heavy molecules and their subsequent condensation to form coke. In addition, SAPO-11 mainly possesses weak acid Lewis sites, which are known to be active for the dehydration of methanol without promoting the formation of coke [126,127].

Nano-sized SAPO-11 with improved properties was synthetized by Chen et al. [126] by the solvothermal-assisted (a seed-induced) process. The catalyst synthetized by this method had nano-sized particles (average size about 200 nm), which implies a decrease in acidity and an increase in the specific surface and mesoporosity between crystals. As a result of improved diffusion, the nano-sized SAPO-11 showed better activity in the dehydration of methanol than γ-Al_2O_3 and micro-SAPO-11 [126]. Catizzone et al. [103] analyzed the effect of the topology and channel size of some zeolites and the SAPO-34 on the DME production from methanol dehydration at 200–240 °C. Zeolites showed a higher methanol conversion and DME selectivity, although the topology and channel size influenced the catalysts' stability and coke formation. 1-D zeolites with open structures and side pockets exhibited an important deactivation due to the high formation of coke deposits. On the other hand, ZSM-5 zeolite channels with a 3-D topology and medium pore size showed lower coke formation. For the SAPO-34 that contains large channel intersections and narrow openings, the deactivation was also pronounced as the large molecules remained in the channels blocking the pores.

The application of silicoaluminophosphate (SAPO) catalysts as acids in the direct synthesis of DME from CO_2 was intensively studied by Bilbao and co-workers [63,127]. SAPO-based catalysts are industrially used for the conversion of methanol, and their activity depends heavily upon their physical characteristics, such as crystal size and morphology. Sánchez-Contador et al. [127] tested SAPO-11, SAPO-18, and HZSM-5 zeolites with different acid characteristics, whereas Ateka et al. [63] used SAPO-18 as an acid function in combination with CuO-ZnO-ZrO_2 and CuO-ZnO-MnO catalysts. The SAPO-11 sample displayed a DME yield higher than 80%. The acid sites' density and their optimized strength were found to be key factors favoring the selectivity toward DME instead of the

formation of the hydrocarbons. Moreover, the 2-D pores' framework made the formation of polyaromatic coke species difficult [127].

Natural clays have also been studied as catalysts for methanol dehydration [27], due to their porosity and tunable Lewis and Brønsted acidity. The representative example is the use of diatomite, porous natural clay, investigated by Pranee et al. [128]. This natural clay with a silica-alumina skeleton was treated with different acids (H_2SO_4, HCl, and HNO_3). A relationship was found between the aluminum ions coordination in the clay and methanol conversion [128]. It was discovered that the methanol dehydration rate increased with the amount of Al(IV) ions in the pre-treated clay. The Al (IV) ions were more active to methanol dehydration than Al (V) and Al (VI) ions. After modification with sulfuric acid, the clay exhibited a high selectivity toward DME (≈99% at 250–350 °C), a diminished adsorption of water molecules, and an inhibition of secondary reactions [128]. The development of SO_4^{2-}-ZrO_2 acid catalysts admixed with CuO-ZnO-ZrO_2 for the direct synthesis of DME via CO_2 hydrogenation was also investigated [129,130]. The yields of DME from the direct hydrogenation of CO_2 over SO_4^{2-}-ZrO_2 were higher than those over the benchmark H-ZSM-5, but the stability of the former catalyst was poorer [129].

WO_x/Al_2O_3 acid catalysts were also studied as acid components in bifunctional catalysts applied in the direct synthesis of DME from CO_2 [131]. The WO_x/Al_2O_3 catalysts were prepared by impregnation of alumina supports with different amounts of W [131,132]. As expected, the experimental results demonstrated that the catalyst activity was determined by both the pore size of Al_2O_3 and the W surface dispersion. The catalyst with small pores and WO_3 nanoparticles on the support surface exhibited the maximum yield of DME. The yields of DME exhibited a volcano curve trend as a function of W surface density. The improvement of the alcohol dehydration rate with the increase in WO_x surface density was attributed to the higher acidity and the formation of Brønsted acid sites as it was proposed by Macht et al. [133]. This is in good agreement with the study of Ladera et al. [134], which demonstrated that there is a relationship between the catalytic performance of the WO_x/TiO_2 catalysts in dimethyl ether formation via methanol dehydration and the acid properties of the catalysts. It was found that the increase in the surface density of W led to an increase in stronger Lewis and Brønsted acid sites derived by the structure density of the W species that defined the molecular structure of WO_x surface species [134].

As a final example of another acid catalyst active and selective for the methanol dehydration, Nb-doped TiO_2 materials can be pointed out in which the acidity can be tuned with the Nb loading [135]. In these systems, the activity of the Nb-doped TiO_2 catalysts increases with the Nb content, which was linked to the higher strength of Lewis acid sites and the increase in the amount of Brønsted acid sites. Interestingly, the catalysts' characterization by the temperature-programmed desorption of NH_3 demonstrated that the amount of Lewis acid sites decreases with Nb content, but their strength follows the opposite trend. It was concluded that the catalytic activity in the methanol dehydration reaction is governed by the strength of acid sites and the presence of Brønsted acid sites, with the catalysts, which are more active, having strong-strength acid sites and possessing a higher amount of Brønsted acid sites.

4. Methods of Preparation of Bifunctional/Hybrid Catalysts for Direct Synthesis of DME from CO_2

The optimization of the bifunctional/hybrid catalysts for the direct synthesis of DME requires a clear strategy in their design and preparation. First, the catalytic functions for methanol synthesis and for methanol dehydration should have adequate kinetic characteristics to work under reaction conditions for the direct synthesis of DME from CO_2 (250–280 °C, 20–50 MPa). Second, the metallic and acidic components of the hybrid or bifunctional catalysts should be optimally mixed to obtain the final catalyst with control in the contact between both metal and acid sites.

The catalytic systems currently employed for the direct synthesis of DME from CO_2 are bifunctional or hybrids. Both types of catalysts differ in the contact between acid and metal sites: Bifunctional catalysts possess separate metal and acid sites, whereas an

intimate contact between them exists in hybrid catalysts. The control of the contact between both metal and acid catalysts is one of the key factors determining the efficiency of the catalyst for the direct production of DME [113]. The general scheme of the preparation of bifunctional/hybrid catalysts is shown in Figure 12. Bifunctional catalysts are prepared by the physical or mechanical mixing of the methanol synthesis catalyst (metal function) with the solid acid catalyst, not achieving an intimate contact between both functionalities. By contrast, the contact between the metallic and acid functions is closer in the hybrid catalysts because they are prepared by one-pot synthesis employing chemical methods, such as co-precipitation (sol–gel), sequential precipitation, chemical metal deposition, impregnation, sonochemical-assisted impregnation, and physical sputtering, that allow for a more intimate mixing of the components.

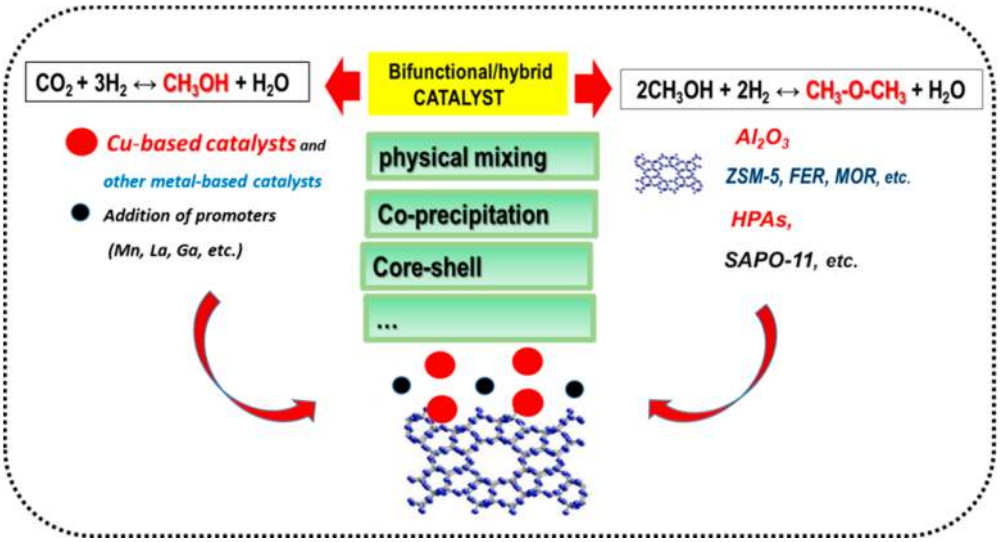

Figure 12. General scheme of the preparation of bifunctional/hybrid catalysts for direct CO_2 hydrogenation to DME.

Whatever the method of preparation used for the preparation of hybrid/bifunctional catalysts, the objective of the preparation is to control the active phases' (metal and acid) dispersion and to control the contact between metal and acid sites. In any case, the use of hybrid/bifunctional catalysts showed a higher DME formation in a single fixed-bed reactor than the DME synthesis on catalysts spatially segregated in two fixed beds [136].

4.1. Precipitation

It is commonly believed that the control in the distribution and size of the active phases is difficult to achieve by employing the co-precipitation method. Despite this, the precipitation method is frequently used for the preparation of bifunctional catalysts applied in the direct synthesis of DME (Figure 13).

For example, the local integration of the methanol-synthesis and methanol-dehydration functionalities was successfully achieved during gel-oxalate co-precipitation of the Cu-Zn-Zr precursors in solutions containing zeolite [137]. Besides the catalyst preparation method, the catalyst chemical composition is crucial to ensure suitable textural and surface properties of Cu-Zn-Zr catalyst [63]. High CO_2 conversion and methanol selectivity were observed on catalysts prepared by the co-precipitation (gel-oxalate) of Cu, Zn, and Zr precursors (Cu loading as high as 57 wt%). By coupling different zeolites with copper-based catalysts via the co-precipitation method, Bonura et al. [138] and Frusteri et al. [104] demonstrated the superiority of FER zeolite over classical MFI, MOR, and Y-type zeolites during CO_2 conversion to DME. An excellent DME production was achieved over Cu-Zn-Zr/FER hybrid systems prepared by the co-precipitation (gel-oxalate) method [104]. The hybrid catalysts prepared by this gel-oxalate co-precipitation method were found to be

very effective catalysts, leading to a final space–time-yield as high as 600 gDME/kg_{cat}/h at 5.0 MPa and 200–260 °C. In those catalysts, the availability of the active sites over the zeolite surface was maximized by controlling the co-precipitation of CuZnZr methanol synthesis precursors. The physicochemical characterization of hybrid catalysts demonstrated that the nature of Cu-ZnO active sites and its surface exposition formed by co-precipitation strongly depends on the morphology of zeolite. In this sense, the morphology of the FER zeolite favors the availability of Brønsted acid sites and it also produces better surface exposition of the Cu-ZnO active sites and the formation of Lewis basic sites for CO_2 activation [104]. The same authors showed new evidence on the interaction between metal and acid sites of H-form FER-type and MFI-type zeolites (Si/Al ratio = 10) on bifunctional CuZnZr/zeolite catalysts prepared via gel oxalate co-precipitation [113]. The catalysts exhibited a good DME yield and resistance to coke formation in the direct CO_2-to-DME reaction carried out at 260 °C and 30 bar because of the adequate crystal size of zeolites (in the range of nanometers) and intimate contact with Cu-Zn sites that favors the mass transfer between the acid and metal sites, leading to a more rapid dehydration of methanol toward DME. In addition, by comparison of the DME selectivity achieved with dual-bed and single-bed reactors, it was concluded that the better efficiency of the bifunctional catalyst is achieved in the case in which intimate interaction between metallic and acid sites is attained [113].

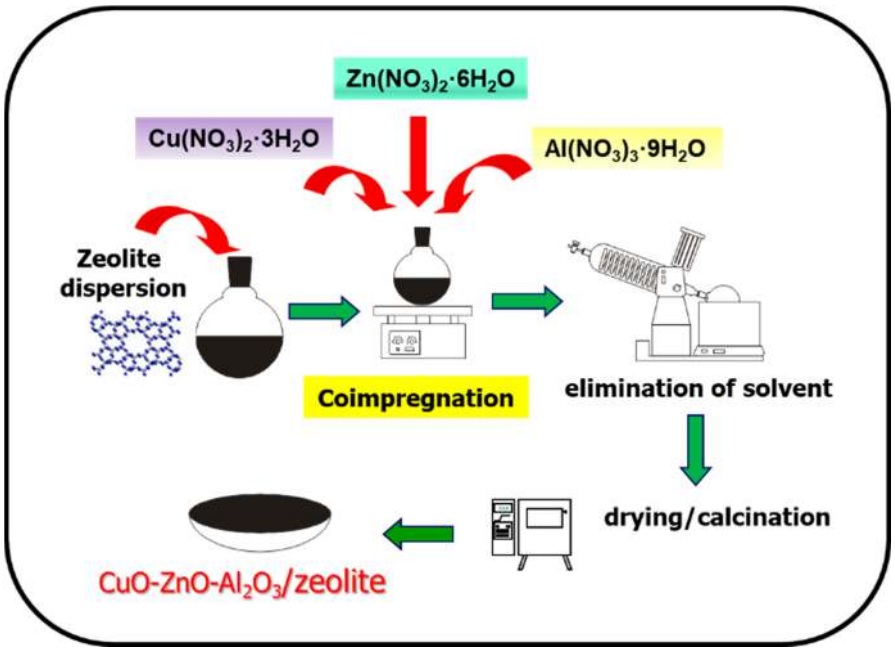

Figure 13. Scheme of the preparation of Cu-ZnO-Al_2O_3/zeolite catalysts for direct synthesis of DME using co-precipitation method.

The importance of the variables in the co-precipitation was demonstrated in the preparation of bifunctional catalysts based on CuO/ZrO_2 and montmorillonite K10 [51]. The metallic CuO/ZrO_2 function was varied by employing different co-precipitation methods: Citric method, and NaOH or Na_2CO_3 methods. Among all synthetized catalysts, the best result in the reaction of CO_2 hydrogenation (a fixed-bed reactor, 40 bar of hydrogen pressure) was obtained with the CuO/ZrO_2 catalyst precipitated using the citric method, because this preparation leads to the better interaction between the metallic and acid sites involved in the process.

Recently, Zhang et al. [139] studied CuO-ZnO-ZrO_2/HZSM-5 hybrids modified with La_2O_3 prepared by co-precipitation. It was found that the catalyst modification with La_2O_3 enhanced its performance in direct CO_2 hydrogenation to DME (270 °C and 30 MPa). Considering the previous study of Guo et al. [140] on the effect of La doping on Cu/ZrO_2 catalysts, this enhancement is associated with an increase in the amount of basic sites that

enhance the adsorption of CO_2 and the selectivity toward methanol formation [140]. The best CO_2 conversion (34.3%) and selectivity toward DME (57.3%) was achieved with the catalyst modified with 1% La_2O_3, which was linked to the optimization of the adsorption of CO_2 and the formation of the smaller Cu active species [139].

The sequential precipitation method was employed by Jeong et al. [141] for the preparation of hybrid Al_2O_3/Cu/ZnO catalysts with different amounts of Al. Using the sequential precipitation method, the complete precipitation of Al^{3+} was achieved using a high concentration of precipitation agent. After calcination, the catalyst with the highest Al content and acidity exhibited the best performance in the direct CO_2 conversion to DME (CO_2 conversion of 25% and DME selectivity of 75% at 300 °C and 50 bar, close to equilibrium values).

4.2. Physical Mixing

The most used method for the combination of metallic and acid catalytic functions in catalysts for the direct synthesis of DME is the physical mixing [136]. The hybrid catalysts prepared by the physical mixing of CuZnAlZr, CuZnZr, or CuZnAl with HZSM-5 or γ-Al_2O_3 exhibited a higher DME formation in a single fixed-bed reactor than the methanol synthesis and solid acid catalysts spatially segregated in two fixed beds [136]. Among the physical mixtures, the results suggest that the HZSM-5 is the more effective acid component than γ-Al_2O_3 [104]. In addition, within the hybrid catalysts with HZSM-5, those mixed with the quaternary CuZnAlZr work better than ternary CuZnZr or CuZnAl catalysts, reaching a STY close to 400 gDME/kg_{cat}/h. The results presented by Jiang et al. [142] provided an understanding of the differences in the nature and strength of the metal–acid interaction in the hybrid catalysts prepared by co-precipitation and physical mixing methods. The hybrids were formed by the metallic Cu/ZnO-ZrO_2 catalyst in combination with an amorphous mesoporous aluminosilicate substrate as an acid catalyst for methanol dehydration (Figure 14). It was found that the physical mixing of the CuO-ZnO-ZrO_2 catalyst with aluminosilicate led to a higher DME production (41 g $kg_{cat}{}^{-1}$ h^{-1} at 260 °C and 20 bar) than in the case of the co-precipitated counterpart [142]. The lower activity observed in the case of the sample prepared by co-precipitation is due to the close contact between the Cu and the Brønsted acid sites that allows for the stabilization of Cu nanoparticles and their incorporation into the siliceous structure losing the active Cu-ZnO contacts. The hydroxyl sites associated with the incorporation of Al atoms into the framework of aluminosilicate act as anchoring sites for Cu species as confirmed by theoretical DFT simulations.

The bifunctional CuO-ZnO-Al_2O_3/HZSM-5 catalyst modified with different promoters (Zr, Mg, Ce, Y) prepared by physical mixing were studied by Lu et al. [143]. The methanol synthesis catalysts were prepared from hydrotalcite-like precursors formed by the simultaneous co-precipitation of Cu, Zn, Al, and the promoter ions (Zr, Mg, Ce, Y). The promoted bifunctional catalysts show high activity in the direct synthesis of DME at 260 °C and 30 bar. The best results were obtained with the catalyst modified with Y achieving a CO_2 conversion of 40.7% and selectivity toward a DME of 54.7%.

Physical mixing of the Cu-Fe-Ce and Cu-Fe-La catalysts with HZSM-5 was investigated by Qin et al. in the direct synthesis of DME from CO_2 [144]. The Cu-Fe-Ce and Cu-Fe-La methanol synthesis catalysts were prepared by the homogeneous precipitation of three metal precursors and mechanically mixed with HZSM-5 zeolite to obtain the bifunctional catalysts. As compared with the Cu-Fe-La catalyst, the Cu-Fe-Ce catalyst was found to be more active and selective toward DME, which was ascribed to a greater specific surface area and lower CuO crystallite size. However, under the reaction conditions employed (T = 260 °C, P = 30 bar), the activity of the Cu-Fe-Ce/HZSM-5 catalyst was relatively low: CO_2 conversion of 18.1% and DME selectivity of 52%.

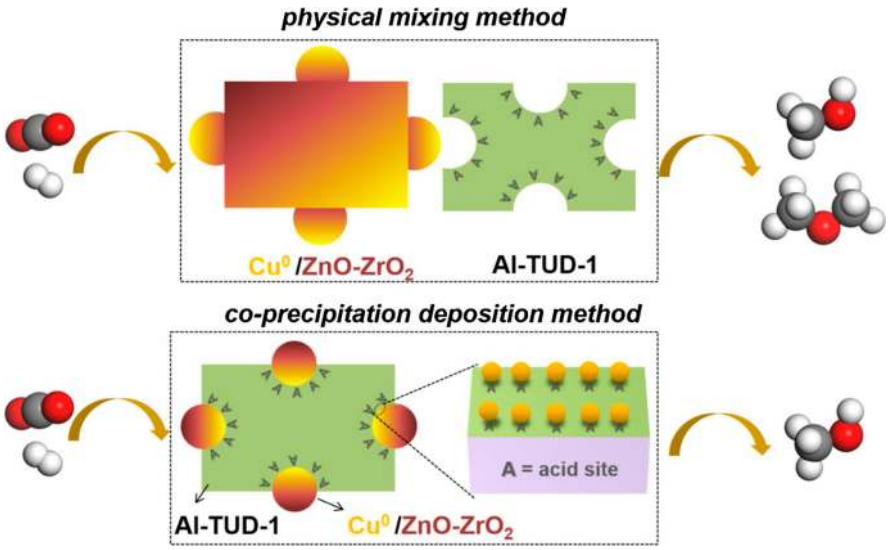

Figure 14. Schematic visualization of hybrid catalysts based on CuO-ZnO-ZrO_2 + mesoporous alumino-silicate prepared by the physical mixing method and co-precipitation deposition (reproduced from [142] with permission from Elsevier License No 5015270559789).

A series the hybrid catalysts formed by CuO-ZnO-ZrO_2 and CuO-ZnO-MnO as a metallic function and SAPO-18 as an acid function were prepared by physical mixing in the study performed by Ateka et al. [63]. The bifunctional catalysts were active for the direct synthesis of DME from CO_2 at 175–250 °C. The bifunctional SAPO-18-based catalysts exhibited better catalytic performance than the γ-Al_2O_3-based counterpart, which was associated with their greater amount of acid sites, the presence of strong acid sites, and its low affinity to adsorb water molecules on the acid sites. Although the CuO-ZnO-ZrO_2/SAPO-16 catalyst exhibited higher CO_2 conversion, the lower preparation cost of the CuO–ZnO–MnO/SAPO-18 catalyst could be an incentive for the use of Mn as a dopant [63].

Interesting results were obtained by using $SrCrCO_3$ as an additive of bifunctional catalysts formed by CuZnAl combined with ZSM-5 [68]. The catalysts were prepared using the $SrCrCO_3$ as a carrier of the CuZnAl catalyst previously prepared by the hydrothermal method, and physically mixed with H-ZSM-5 zeolite. The CO_2 conversion and yield of DME on these bifunctional catalysts were relatively high, 30.3% and 27.8%, respectively. The catalyst was relatively stable during 150 h of reaction time and only a small decrease in activity was observed. The enhancement of activity was linked to changes in the catalyst structure due to the formation of a tridimensional frame that facilitates the access to the acid sites and also the modification of the Cu methanol active sites by electron transfer with the $SrCrO_3$ additive [68].

4.3. Nanostructuration (Core–Shell Capsule Catalysts)

Conventional methodologies (precipitation and physical mixing) do not allow the fine control of the size and distribution of active metal and acid sites, producing catalysts that exhibit an open structure for the access of CO_2 and H_2 to the active sites. This kind of structure makes it difficult the control the product selectivity in the reaction of CO_2 hydrogenation. In this sense, the catalyst selectivity can be more controlled by assembling the metal and acid functions of the hybrid catalyst into the nanostructures such as the core–shell-structured capsule catalyst. The space-confined reaction environment associated with the structured capsule catalyst could favor the control of the selectivity to DME in the direct hydrogenation of CO_2 [145,146]. In addition, the bifunctional nanostructured capsule catalysts enhance the synergetic effect between metal and acid sites and allow some changes in their surface properties (hydrophobicity). In fact, capsule catalysts demonstrated excellent catalytic performance in the tandem syngas-methanol-DME reactions, and therefore, they are also promising for direct DME production via CO_2 hydrogenation.

Recent developments in the design of multifunctional capsule catalysts and their use in heterogeneous catalytic reactions were recently reviewed by Bao and Tsubaki [147], and Gao et al. [146].

A schematic visualization of the direct CO_2 hydrogenation on a bifunctional capsule catalyst is shown in Figure 15. In this scheme, methanol synthesis occurs in the core of the catalyst (metal function), while methanol dehydration occurs in the shell around this core (acid function). In the one-step DME synthesis from CO_2 and H_2 using the capsule catalyst, the "synergy" of the chemical transformation was combined with the heat transfer from the core catalyst to the zeolite shell. The capsule catalyst can be prepared employing various methods, such as the dual-layer method, hydrothermal synthesis, single-crystal crystallization, or physically adhesive method. However, zeolite shell preparation needs high temperature and alkaline pH, limiting its application in combination with Cu/ZnO methanol synthesis catalysts. Using the hydrothermal method for the zeolite synthesis, it is easy to lose the active phase of the core Cu/ZnO methanol synthesis catalyst during the zeolite shell incorporation [145]. This core corrosion can be avoided using the methods proposed by Bao and Tsubaki [145] for the zeolite shell incorporation: A direct liquid membrane crystallization method and a dual-layer synthesis approach under a close-to-neutral condition.

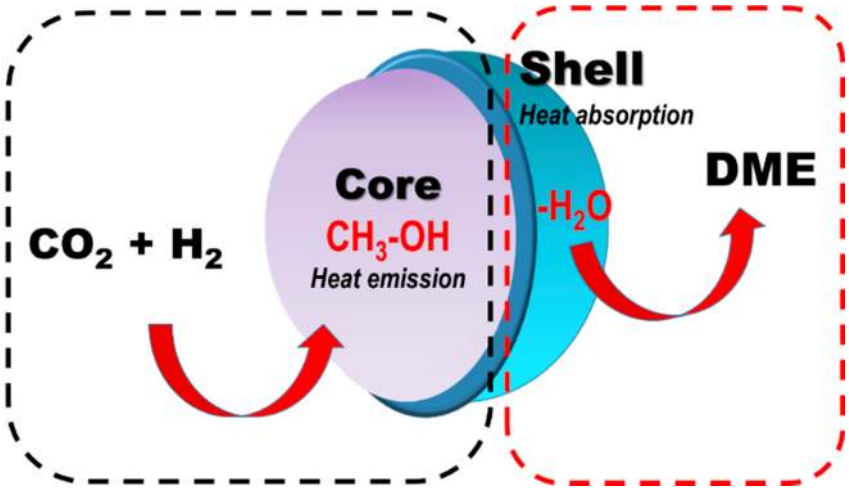

Figure 15. Illustration of direct CO_2 hydrogenation on a bifunctional capsule catalyst.

The first tailor-made bifunctional capsule catalyst for direct synthesis of DME had $Cu/Zn/Al_2O_3$ in the core and H-ZSM-5 in the zeolite shell [147,148]. The micro-sized H-ZSM-5 shell was prepared using two different methods: The conventional synthesis of H-ZSM-5 zeolite and a close-to-neutral silicate-1 zeolite synthesis method in which the core catalyst is used simultaneously as the aluminum supplier. In the latter method, the aluminum migrated from the core $Cu/Zn/Al_2O_3$ catalyst was incorporated into the zeolite framework forming the interface between the zeolite shell and the core catalyst [147,148]. The activity results showed that the capsule catalyst prepared by close-to-neutral silicalite-1 zeolite synthesis exhibited a significantly improved activity with respect to the counterpart prepared using the hydrothermal method [147,148]. This is because, contrary to the hydrothermal method, the aluminum migration method favors the formation of the defect-free zeolite shell.

The relatively simple and scalable physical coating method was employed by Phienluhon et al. [149] for the preparation of the zeolite CuZnAl/SAPO-11 capsule catalyst without hydrothermal synthesis. This catalyst possesses $Cu/ZnO/Al_2O_3$ in its core structure and silicoaluminophosphate SAPO-11 in its shell. The catalyst activity was considerably better than that of the same catalyst prepared by physical mixing. The excellent catalytic performance of the CuZnAl/SAPO-11 capsule catalyst was explained as due to its core–shell-like structure that favors the syngas conversion to DME and suppresses the

over-dehydration of DME to by-products [149]. A reverse capsule formed by a core of Cu/Al_2O_3 for methanol synthesis and a shell of Al_2O_3 for methanol dehydration was prepared by Tan et al. [150] by the surface infiltration method. Owing to well-matched reactions of methanol synthesis on the Cu-Al_2O_3 shell and its dehydration to DME on the Al_2O_3 core, the catalyst exhibited a much higher CO_2 conversion and DME selectivity than the conventional powdered Cu/Al_2O_3 catalyst [150].

The effect of the silica precursor (tetraethyl orthosilicate (TEOS) and sodium metasilicate (SMS)) on the catalytic behavior of the hybrid capsule Cu/Zr-SBA-15 catalyst was studied by Atakan et al. [151]. The Cu nanoparticles were deposited on the Zr-SBA-15 carrier by the infiltration or wetness impregnation method. From the activity–structure correlation, it was concluded that the type of silica precursor and Cu loading method affected the catalytic activity and selectivity, respectively. Better activity results were obtained with the catalyst prepared using TEOS as the silica precursor. This was linked to the more favorable Zr dispersion and its bonding to the silica surface. Interestingly, it was found that Cu incorporation by evaporation and infiltration-induced wetness impregnation favored the selectivity for the synthesis of methanol and methanol dehydration to DME, respectively, which was ascribed as due to the higher Zr content and better reducibility of Cu on the catalysts prepared by impregnation of Cu [151].

4.4. Other Methods (CVD and Grafting)

Eschewing the common use of Cu-based catalysts for DME production, there are few works exploring the catalytic use of noncopper-based systems for direct CO_2 hydrogenation to DME [152]. These works are mainly focused on the use of PdZn alloy nanoparticles as active sites for methanol synthesis. For example, Bahruji et al. [152] studied the deposition of PdZn alloy nanoparticles onto ZSM-5 zeolite via the chemical vapor impregnation method. This hybrid catalytic system exhibited a dual functionality: The PdZn alloy for the CO_2 hydrogenation to methanol and the ZSM-5 zeolite for the methanol dehydration to DME. In the reaction at 270 °C, the hybrid catalyst exhibited a high DME synthesis rate (546 mmol kg_{cat}^{-1} h^{-1}). Interestingly, its catalytic behavior was similar to that of the catalyst prepared by the physical mixing of the metallic component (5% Pd-15% Zn/TiO_2) with acidic zeolite (H-ZSM-5) [152]. However, the TiO_2-containing catalyst prepared by physical mixing produced higher yields of oxygenated products than the PdZn/ZSM-5 catalyst prepared by the chemical vapor deposition method [152]. The comparison of the catalytic behavior of PdZn and H-ZSM-5 catalysts prepared by physical mixing and by chemical vapor impregnation (surface organometallic chemistry grafting) demonstrated that the contact achieved in the sample prepared by physical mixing improves the functionality and efficiency of the hybrid catalyst [153]. Besides the formation of the PdZn alloy phase in both catalysts, the catalyst prepared by physical mixing was more active in CO_2 hydrogenation than its grafted analog. From the catalyst characterization, it was concluded that the lower activity of the latter catalyst was due to the exchange of Brønsted acid sites in H-ZSM-5 by Zn(II), leading to the formation of inactive species.

5. Status on Catalyst Development for Direct Synthesis of DME from CO_2

There are many factors influencing the catalytic activity of the bifunctional/hybrid catalysts for direct synthesis of DME. As stated above, they are hugely affected by the catalyst preparation method because it determines the porosity, active metal surface area, acid strength and nature, as well as distribution and contact between both functionalities [154]. The comparison of catalysts prepared in different laboratories is difficult due to the different chemical compositions of catalysts and the reaction conditions used in their testing. Among the different catalytic systems explored so far in the direct DME synthesis from CO_2, Table 2 shows a comparison among the most active catalysts formulations based on Cu catalysts with similar metal-to-acid weight ratios (around 2) and tested under similar reaction conditions. The results presented in Table 2 show that the best performance and selectivity toward DME were obtained using CuO-ZnO-Al_2O_3/ZSM-5 catalyst formula-

tion [155,156]. Using this catalyst formulation, the higher DME yield was obtained for the catalyst prepared by co-precipitation followed by the mechanical mixing of both methanol synthesis and methanol dehydration catalysts [155] than for the bifunctional catalyst prepared by gel oxalate co-precipitation in solution containing finally dispersed zeolite [156]. The excellent catalytic behavior of this catalyst was attributed to its microstructure formed during the catalyst preparation. The deactivation of this catalyst during 100 h was relatively high: The CO_2 conversion decreased from 25.6% to 21.4%. The catalyst deactivation was due to coking, Cu sintering, and the decrease in the specific surface area. The DME yield of the CuO-ZnO-Al_2O_3/ZSM-5 catalyst prepared by co-precipitation and physical mixing by Hu et al. [156] was significantly higher than that reported for the catalytic system prepared by a fast urea–nitrate combustion method and then mixed physically with HZSM-5 (18.5% against 15.1%) [154]. Therefore, besides the chemical composition and mixing method, the method selected for the preparation of the methanol synthesis catalyst has a great influence on the final DME production. Besides this, the importance of the metal-to-acid mass ratio is obvious when comparing the activity results of the CuO-ZnO-ZrO_2/HZSM-5 catalyst prepared with different metal/acid ratio [157]. The lower activity of the catalysts with high metal/acid ratio with respect to other catalysts prepared with the mass ratio of 1:1 (Table 2) can be most likely due to its small acid function. Finally, the comparison of the efficiency of bifunctional and hybrids tested under similar experimental conditions (5 MPa and 260 °C) demonstrated that physical mixtures of mixed oxides and acidic materials exhibited a lower DME yield than hybrid single-grain catalysts [104].

Table 2. Activity of selected hybrid and bifunctional catalysts based on Cu for direct DME synthesis from CO_2.

Catalyst [a]	Preparation Method [d]	GHSV (mL g^{-1} h^{-1})	T (°)	P (bar)	X_{CO2} (%)	S_{DME} (%)	Yield DME (%)	Ref.
CuO-ZnO-Al_2O_3/ZSM-5	(A)	1525	260	42	30.5	72.0	21.9	[155]
CuO-ZnO-ZrO_2-La_2O_3(1%)/ZSM-5	(B)	4200	270	30	34.3	57.3	19.6	[139]
CuO-ZnO-Al_2O_3/ZSM-5	(B)	1500	260	30	27.3	67.1	18.3	[156]
CuO-ZnO-Al_2O_3/ZSM-5	(C) [b]	3600	250	30	21.3	63.4	13.5	[157]
CuO-ZnO-Al_2O_3/ZSM-5	(D)	4200	270	30	30.6	49.2	15.1	[154]
CuO-ZnO-Al_2O_3/ZSM-5	(B)	8800	260	30	21	35	7.4	[158]
CuO-ZnO-ZrO_2/FER	(E)	8800	280	50	29	62	18.0	[138]
CuO-ZnO-ZrO_2/MOR	(E)	8800	280	50	26	51	13.0	[138]
CuO-ZnO-ZrO_2/ZSM-5	(B)	8800	260	50	21	41	8.6	[104]
CuO-ZnO-Ga_2O_3/ZSM-5	(B)	8800	260	30	21	36	7.6	[158]
CuO-ZnO-La_2O_3/FER	(B)	8800	260	30	18	34	6.1	[158]
CuO-ZnO-CeO_2/FER	(B)	8800	260	30	14	36	5.0	[158]
CuO-ZrO_2 + K10 [c] +3% Mn	(F)	1800	260	40	7	22	1.5	[51]
CuO-ZrO_2 + K10 [c] + 3% Ga	(F)	1800	260	40	7	20	1.4	[51]
Cu-Fe-La/ZSM-5	(G)	1500	260	30	17.2	51.3	8.8	[144]
Cu-Fe-Ce/ZSM-5	(G)	1500	260	30	18.1	52.0	9.4	[144]

[a] Metal-to-acid phase weight ratio of 1. [b] Metal-to-zeolite weight ratio of 10. [c] K10: Montmorillonite. [d] Method of the catalyst preparation: (A) Co-precipitation + mechanical mixing with zeolite; (B) gel oxalate co-precipitation in solution containing finally dispersed zeolite; (C) solid state reaction + physical mixing with zeolite (metal-to-zeolite weight ratio of 10); (D) combustion route + physical mixing with zeolite; (E) co-precipitation in zeolite solution; (F) co-precipitation by NaOH + physical mixing with zeolite; (G) homogeneous co-precipitation + mechanical mixing with zeolite.

Despite the advances in the development of catalysts with high activity and selectivity to DME, an important challenge in the catalytic behavior of the bifunctional/hybrid catalysts for direct DME from CO_2 is the prevention or limitation of deactivation. The

hybridized bifunctional catalysts can be deactivated by the detrimental interaction between the metal and acid sites, such as ion exchange between hydrogenation and dehydration catalysts. The deactivation during long-term testing was demonstrated by Ren et al. [155] for the CuO-ZnO-ZrO_2-Al_2O_3/ZSM-5 (CZZA/ZSM-5) catalyst tested in direct CO_2 hydrogenation to DME. A significant decrease was observed in the specific BET surface area and an increase in coke in the spent CZZA/ZSM-5 catalyst after 100 h of DME synthesis. Therefore, it was concluded that the presence of zeolite has a detrimental effect on the catalyst stability. Observed changes in the structural properties of the catalyst (e.g., the specific BET surface area and crystallinity) suggested that zeolite-induced coking might be responsible for deactivating the catalyst. In particular, the dehydration of methanol to DME favors the formation of methane and coke as by products [156,157]. The formation of methane occurs due to the strong bonding of methoxy species on the acid sites, leading to the formation of surface formats, that decompose forming CO, H_2, and CH_4 [89]. Long-term tests on CuO-ZnO-Al_2O_3/ZSM-5 hybrid bifunctional catalysts also show deactivation.

As discussed in Section 2, the hydrogenation of CO_2 led to the formation of a high concentration of H_2O in the reaction medium. Water generated can be adsorbed on the bifunctional hybrid catalysts, which could accelerate its deactivation, such as the ion exchange between hydrogenation and dehydration catalysts. The study by Frustrei et al. [104] showed that a progressive deactivation of the CuZnZr-FER catalyst in the direct hydrogenation of CO_2 to DME was not due to the deposition of coke or sintering of metals, but mainly to the formation of water. The adsorption of H_2O on the catalyst surface negatively affected the functionality of the metal and acid catalysts [104,158]. In this sense, the FTIR characterization of the fresh and spent Cu-ZnO-ZrO_2/ferrierite catalysts indicated that the loss of activity in the bifunctional catalyst in the CO_2-methanol-DME reaction can be related to acidity loss due to H^+/Cu^{2+} ion exchange and the sintering of Cu particles, leading to a decrease in the CO_2 hydrogenation toward methanol [159]. To increase the water resistance of hybrid catalysts, the use of ZrO_2 as a promoter is a good solution, because zirconium oxide showed excellent water tolerance and could also prevent the water-induced growth of the CuO_x crystals [157]. In fact, a long-term stability test indicated that the ZrO_2-modified hybrid had superior stability during methanol and DME synthesis, as compared to the ZrO_2-free hybrid counterpart [157]. However, the DME yield achieved in the ZrO_2-modified hybrid catalyst was low (18.3% at 240 °C and 27.6 bar). Despite the improvements in the stability achieved with the ZrO_2 addition, the low product yield achieved has been a significant challenge in this type of bifunctional catalyst.

Therefore, it can be concluded from the studies published in the literature that the development of hybridized/bifunctional catalysts has achieved remarkable improvements in catalysts with high activity and selectivity in the transformation of CO_2 to DME. However, the stability of the catalysts for CO_2 hydrogenation has not been sufficient, and therefore, more research is needed for the development of new bifunctional/hybrid catalysts that show better performance in terms of stability toward the fast deactivation induced by water generated during the hydrogenation of CO_2 toward methanol.

6. Conclusions and Future Perspectives

Dimethyl ether is a very promising fuel and chemical molecule whose direct synthesis from CO_2 has been attracting considerable interest in recent years because of the higher efficiency and lower operational costs with respect to the conventional two-step syngas process. However, the direct synthesis of DME from CO_2 has significant kinetics and thermodynamic limitations that require the development of effective hybrid/bifunctional catalysts. For catalyst design, this process is challenging, because to obtain a good synergy between both functionalities, it is necessary to control their nature, balance, contact, and distance between the metal and acid site. Despite the strong requirements for catalyst development, this review demonstrated that there is great progress in the development of hybrid/bifunctional catalysts for the direct conversion of CO_2 to DME. To date, a large number of bifunctional catalysts have been studied for the direct synthesis of DME from

CO_2 reaching conversion and DME selectivity values of 20–30%, and 20–70%, respectively. Among the hybrid/bifunctional formulations studied to date, the combination of Cu/ZnO with H-ZSM-5 stands out as most effective in terms of its optimal activity/cost ratio. Despite the progress achieved, important advances in the development of bifunctional catalysts must be made in terms of activity and, most importantly, resistance to deactivation by water.

Despite the large number of catalyst formulations explored for the synthesis of methanol from CO_2, those based on Cu/ZnO systems are most widely used. Cu/ZnO catalysts should be optimized for this application, and issues related to the improvement in its low-temperature activity, deactivation behavior with water, and selectivity to CO need to be solved. Making smaller Cu particles by new synthesis strategies, improving the interaction of Cu-ZnO by ZnO doping, and increasing the defects of the Cu phase are excellent strategies to develop successful CO_2 hydrogenation catalysts based on Cu-ZnO. Novel catalysts are expected to be developed and, among the alternative formulations explored to date, those based on Pd and In_2O_3 have the greatest potential to overcome the limitations observed in the most widely used catalysts based on the classic Cu-ZnO system.

New acid catalysts are expected to be developed with an optimized number, nature, and strength of acid sites (Brønsted/Lewis) to obtain high dehydration activities at low temperatures compatible with the thermodynamically more favorable conditions for the methanol synthesis step. As the Lewis acid sites are reported to be more active than Brønsted counterparts for methanol dehydration, improvement in hybrid catalysts for DME production should be made by an increased amount of Lewis acid sites. In this sense, it is necessary to investigate the possible interconversion of Lewis/Brønsted sites in the presence of water.

As shown in this literature survey, the strategies for the preparation of hybrids/bifunctional catalysts are core aspects in the control of the dispersion and the contact between metal and acid sites, and they determine the final activity and selectivity of the catalysts. Conventional methodologies (precipitation and physical mixing) used in most of the analyzed studies do not allow fine control of the size and distribution of active metal and acid sites, and produce catalysts that exhibit an open structure for the access of CO_2 and H_2 to the active sites. This kind of structure makes the control of the product selectivity difficult in the reaction of CO_2 hydrogenation. Structured hybrid/bifunctional catalysts with a space-confined reaction environment in the form of a capsule or core–shell could improve both the selectivity to DME and the stability. Therefore, the nanostructuration in the form of a capsule or core–shell should be more deeply investigated as an efficient strategy to obtain a good synergy between both functionalities and to avoid their partial deactivation in direct DME synthesis.

In summary, a broader adoption of direct CO_2-to-DME synthesis technology requires significant progress in the development of bifunctional catalysts in terms of activity, selectivity, and most importantly, resistance to water deactivation. In this sense, advanced spectroscopic "operando" techniques could be very useful in elucidating the structure and interaction between metal and acid sites in working conditions. The information obtained from these techniques could help us to understand the mechanisms that operate in the selective hydrogenation of CO_2 to DME and the process involved in the deactivation of active sites. In addition, this information is needed to design catalysts that have maximized the number of active/selective catalytic sites for DME synthesis under working conditions.

Author Contributions: Conceptualization, R.M.N.; methodology, N.M. and E.M.O.; validation, resources, N.M.; data curation, N.M.; writing—original draft preparation, J.L.G.F. and B.P.; writing—review and editing, R.M.N.; visualization, E.M.O.; supervision, R.M.N. All authors have read and agreed to the published version of the manuscript.

Funding: The present investigation was performed within the research programs CTQ2016-76505-C3-1 and PID2019-111219RB-100 supported by the Spanish Ministry of Science, Innovation and Universities. The Autonomous Community of Madrid (CAM) is also gratefully acknowledged for

funding the BIOTRES-CM (P2018/EMT-4344) project. Elena Millán would like to acknowledge the FPI program from the Spanish Ministry of Science, Innovation and Universities for the research grant.

Data Availability Statement: Data sharing is not applicable to this article.

Conflicts of Interest: The authors declare no conflict of interest.

References

1. World Energy Outlook 2020, IEA, Paris. Available online: https://www.iea.org/topics/world-energy-outlook (accessed on 13 September 2019).
2. Global CO2 Emissions in 2019, IEA 2020, Paris. Available online: https://www.iea.org/articles/global-CO2-emissions-in-2019 (accessed on 10 July 2019).
3. Long-term low greenhouse gas emission development strategy of the EU and its Member States. Available online: https://ec.europa.eu/clima/policies/strategies/2050_en (accessed on 12 April 2019).
4. CO_2 Value Europe. Available online: http://www.co2value.eu/ (accessed on 23 March 2021).
5. Styring, P.; Jansen, D.; de Coninck, H.; Reith, H.; Armstrong, K. *Carbon Capture and Utilisation in the Green Economy*; The Centre for Low Carbon Futures: York, UK, 2011.
6. Kerry Yu, K.M.; Yu, P.K.M.; Curcic, I.; Gabriel, J.; Tsang, S.C.E. Recent advances in CO_2 capture and utilization. *ChemSusChem* **2008**, *1*, 893–899. [CrossRef]
7. Markewitz, P.; Kuckshinrichs, W.; Leitner, W.; Linssen, J.; Zapp, P.; Bongartz, R.; Schreiber, A.; Müller, T.E. Worldwide innovations in the development of carbon capture technologies and the utilization of CO2. *Energy Environ. Sci.* **2012**, *5*, 7281–7305. [CrossRef]
8. Von der Assen, N.; Jung, J.; Bardow, A. Life-cycle assessment of carbon dioxide capture and utilization: Avoiding the pitfalls. *Energy Environ. Sci.* **2013**, *6*, 2721–2734. [CrossRef]
9. Dena Study Integrated Energy Transition, Deutsche Energie-Agentur GmbH (dena), Berlin, Germany. 2018. Available online: https://t.co/8pKe0xiDXz (accessed on 23 March 2021).
10. Song, C. Global challenges and strategies for control, conversion and utilization of CO_2 for sustainable development involving energy, catalysis, adsorption and chemical processing. *Catal. Today* **2006**, *115*, 2–32. [CrossRef]
11. Neelis, M.; Patel, M.; Blok, K.; Haije, W.; Bach, P. Approximation of theoretical energy-saving potentials for the petrochemical industry using energy balances for 68 key processes. *Energy* **2007**, *32*, 1104–1123. [CrossRef]
12. Marchionna, M.; Patrini, R.; Sanfilippo, D.; Migliavacca, G. Fundamental investigations on di-methyl ether (DME) as LPG substitute or make-up for domestic uses. *Fuel Process. Technol.* **2008**, *89*, 1255–1261. [CrossRef]
13. Fleisch, T.H.; Basu, A.; Sills, R.A. Introduction and advancement of a new clean global fuel: The status of DME developments in China and beyond. *J. Nat. Gas Sci. Eng.* **2012**, *9*, 94–107. [CrossRef]
14. Nasser, G.; Kurniawan, T.; Miyake, K.; Galadima, A.; Hirota, Y.; Nishiyama, N.; Muraza, O. Dimethyl ether to olefins over dealuminated mordenite (MOR) zeolites derived from natural minerals. *J. Nat. Gas Sci. Eng.* **2016**, *28*, 566–571. [CrossRef]
15. Haro, P.; Trippe, F.; Stahl, R.; Henrich, E. Bio-syngas to gasoline and olefins via DME-A comprehensive techno-economic assessment. *Appl. Energy* **2013**, *108*, 54–65. [CrossRef]
16. Liu, Y.; Murata, K.; Inaba, M.; Takahara, I. Synthesis of ethanol from methanol and syngas through an indirect route containing methanol dehydrogenation, DME carbonylation, and methyl acetate hydrogenolysis. *Fuel Process. Technol.* **2013**, *110*, 206–213. [CrossRef]
17. Saravanan, K.; Ham, H.; Tsubaki, N.; Bae, J.W. Recent progress for direct synthesis of dimethyl ether from syngas on the heterogeneous bifunctional hybrid catalysts. *Appl. Catal. B Environ.* **2017**, *217*, 494–522. [CrossRef]
18. Catizzone, E.; Freda, C.; Braccio, G.; Frusteri, F.; Bonura, G. Dimethyl ether as circular hydrogen carrier: Catalytic aspects of hydrogenation/dehydrogenation steps. *J. Energy Chem.* **2021**, *58*, 55–77. [CrossRef]
19. Zannis, T.C.; Hountalas, D.T. DI Diesel Engine Performance and Emissions from the Oxygen Enrichment of Fuels with Various Aromatic Content. *Energy Fuels* **2004**, *18*, 659–666. [CrossRef]
20. Mondal, U.; Yadav, G.D. Perspective of dimethyl ether as fuel: Part I. Catalysis. *J. CO_2 Util.* **2019**, *32*, 299–320. [CrossRef]
21. Catizzone, E.; Bonura, G.; Migliori, M.; Frusteri, F.; Giordano, G. CO_2 recycling to dimethyl ether: State-of-the-art and perspectives. *Molecules* **2018**, *23*, 31. [CrossRef]
22. Sun, J.; Yang, G.; Yoneyama, Y.; Tsubaki, N. Catalysis chemistry of dimethyl ether synthesis. *ACS Catal.* **2014**, *4*, 3346–3356. [CrossRef]
23. Azizi, Z.; Rezaeimanesh, M.; Tohidian, T.; Reza Rahimpour, M. Dimethyl ether: A review of technologies and production challenges. *Chem. Eng. Process.* **2014**, *82*, 150–172. [CrossRef]
24. Álvarez, A.; Bansode, A.; Urakawa, A.; Bavykina, A.V.; Wezendonk, T.A.; Makkee, M.; Gascon, J.; Kapteijn, F. Challenges in the greener production of formates/formic acid, methanol, and DME by heterogeneously catalyzed CO_2 hydrogenation processes. *Chem. Rev.* **2017**, *117*, 9804–9838. [CrossRef] [PubMed]
25. Liu, M.; Yi, Y.; Wang, L.; Guo, H.; Bogaerts, A. Hydrogenation of carbon dioxide to value-added chemicals by heterogeneous catalysis and plasma catalysis. *Catalysts* **2019**, *9*, 275. [CrossRef]
26. Ye, R.-P.; Ding, J.; Gong, W.; Argyle, M.D.; Zhong, Q.; Wang, Y.; Russel, C.K.; Xu, Z.; Russel, A.G.; Li, Q.; et al. CO_2 hydrogenation to-high-value products via heterogeneous catalysis. *Nat. Commun.* **2019**, *10*, 5698. [CrossRef]

27. Borroso-Martín, I.; Infantes-Molina, A.; Fini, F.J.; Ballesteros-Plata, D.; Rodríguez-Castellón, E.; Moretti, E. Silica-related catalysts for CO_2 transformation into methanol and dimethyl ether. *Catalysts* **2020**, *10*, 1282. [CrossRef]
28. Huang, M.H.; Lee, H.M.; Liang, K.C.; Tzeng, C.C.; Chen, W.H. An experimental study on single-step dimethyl ether (DME) synthesis from hydrogen and carbon monoxide under various catalysts. *Int. J. Hydrog. Energy* **2015**, *40*, 13583–13593. [CrossRef]
29. Wang, Y.; Wang, W.L.; Chen, Y.X.; Zhen, J.J.; Li, R.F. Synthesis of dimethyl ether from syngas using a hierarchically porous composite zeolite as the methanol dehydration catalyst. *J. Fuel. Chem. Technol.* **2013**, *41*, 873–882. [CrossRef]
30. Asthana, S.; Samanta, C.; Bhumik, A.; Banerjee, B.; Voolapalli, R.K.; Saha, B. Direct synthesis of dimethyl ether from syngas over Cu-based catalysts: Enhanced selectivity in the presence of MgO. *J. Catal.* **2016**, *334*, 89–101. [CrossRef]
31. Ateka, A.; Pérez-Uriarte, P.; Gamero, M.; Ereña, J.; Aguayo, A.T.; Bilbao, J. A comparative thermodynamic study on the CO_2 conversion in the synthesis of methanol and of DME. *Energy* **2017**, *120*, 796–804. [CrossRef]
32. Jia, G.; Tan, Y.; Han, Y. A comparative study on the thermodynamics of dimethyl ether synthesis from CO hydrogenation and CO_2 hydrogenation. *Ind. Eng. Chem. Res.* **2006**, *45*, 1152–1159. [CrossRef]
33. Kunkes, E.; Behrens, M. Methanol Chemistry. In *Chemical Energy Storage*; Walter de Gruyter GmbH: Berlin, Germany, 2013; pp. 413–435.
34. Sahibzada, M.; Metcalfe, I.S.; Chadwick, D. Methanol synthesis from $CO/CO_2/H_2$ at differential and finite conversions. *J. Catal.* **1998**, *174*, 111–118. [CrossRef]
35. Liang, B.; Ma, J.; Su, X.; Yang, C.; Duan, H.; Zhou, H.; Deng, S.; Li, L.; Huang, Y. Investigation on deactivation of $Cu/ZnO/Al_2O_3$ catalyst for CO_2 hydrogenation to methanol. *Ind. Eng. Chem. Res.* **2019**, *58*, 9030–9037. [CrossRef]
36. Trenco, G.A.; Vidal-Moya, A.; Martinez, A. Study of the interaction between components in hybrid CuZnAl/HZSM-5 catalysts and its impact in the syngas-to –DME reaction. *Catal. Today* **2012**, *179*, 43–51. [CrossRef]
37. Dasireddy, V.D.B.C.; Neja, S.S.; Blaz, L. Correlation between synthesis pH, structure and $Cu/MgO/Al_2O_3$ heterogeneous catalyst activity and selectivity in CO_2 hydrogenation to methanol. *J. CO2 Util.* **2018**, *28*, 189–199. [CrossRef]
38. Kunkes, E.L.; Studt, F.; Abild-Pedersen, F.; Schlögl, R.; Behrens, M. Hydrogenation of CO_2 to methanol and CO on $Cu/ZnO/Al_2O_3$: Is there a common intermediate or not? *J. Catal.* **2015**, *328*, 43–48. [CrossRef]
39. Liao, F.; Huang, Y.; Ge, J.; Zheng, W.; Tedsree, K.; Collier, P.; Hong, X.; Tsang, S.C. Morphol-ogy-dependent interactions of ZnO with Cu nanoparticles at the materials interface in selective hy-drogenation of CO_2 to methanol. *Angew. Chem. Int. Ed.* **2011**, *50*, 2162–2165. [CrossRef]
40. Kuld, S.; Thorhauge, M.; Falsig, H.; Elkjær, C.F.; Helveg, S.; Chorkendorff, I.; Sehested, J. Quantifying the promotion of Cu catalysts by ZnO for methanol synthesis. *Science* **2016**, *352*, 969–974. [CrossRef]
41. Behrens, M.; Studt, F.; Kasatkin, I.; Kuhl, S.; Havecker, M.; Abild-Pedersen, F.; Zander, S.; Girgsdies, F.; Kurr, P.; Kniep, B.L.; et al. The Active Site of Methanol Synthesis over $Cu/ZnO/Al_2O_3$ Industrial Catalysts. *Science* **2012**, *336*, 893–897. [CrossRef] [PubMed]
42. Álvarez Galván, C.; Schumann, J.; Behrens, M.; Fierro, J.L.G.; Schlögl, R.; Frei, E. Reverse water-gas shift reaction at the Cu/ZnO interface: Influence of the Cu/Zn ratio on structure-activity correlations. *Appl. Catal. B Environ.* **2016**, *195*, 104–111. [CrossRef]
43. Tarasov, A.V.; Seitz, F.; Schlögl, R.; Frei, E. In situ quantification of reaction adsorbates in low temperature methanol synthesis on a high-performance Cu/ZnO:Al catalyst. *ACS Catal.* **2019**, *9*, 5537–5544. [CrossRef]
44. Guil-López, R.; Mota, N.; Llorente, J.; Millán, E.; Pawelec, N.; Fierro, J.L.G.; Navarro, R.M. Methanol synthesis from CO_2: A review of the latest developments in heterogeneous catalysis. *Materials* **2019**, *12*, 3902. [CrossRef] [PubMed]
45. Zhao, Y.F.; Yang, Y.; Mims, C.; Peden, C.H.F.; Li, J.; Mei, D. Insight into methanol synthesis from CO_2 hydrogenation on Cu(1 1 1): Complex reaction network and the effects of H_2O. *J. Catal.* **2011**, *281*, 199–211. [CrossRef]
46. Porosoff, M.D.; Yan, B.; Chen, J.G. Catalytic reduction of CO_2 by H_2 for synthesis of CO, methanol and hydrocarbons: Challenges and opportunities. *Energy Environ. Sci.* **2016**, *9*, 62–73. [CrossRef]
47. Zander, S.; Kunkes, E.L.; Schuster, M.E.; Schumann, J.; Weinberg, G.; Teschner, D.; Jacobsen, N.; Schlögl, R.; Behrens, M. The role of the oxide component in the development of copper composite catalysts for methanol synthesis. *Angew. Chem. Int. Ed.* **2013**, *52*, 6536–6540. [CrossRef]
48. Hansen, J.B.; Nielsen, P.E.H. Methanol synthesis. In *Handbook of Heterogeneous Catalysis*; Ertl, G., Knözinger, H., Schüth, F., Weitkamp, J., Eds.; Wiley-VCH: Winheim, Germany, 2008; p. 1593.
49. Behrens, M.; Zander, S.; Kurr, P.; Jacobsen, N.; Senker, J.; Koch, G.; Ressler, T.; Fischer, R.W.; Schlögl, R. Performance Improvement of Nanocatalysts by Promoter-Induced Defects in the Support Material: Methanol Synthesis over Cu/ZnO:Al. *J. Am. Chem. Soc.* **2013**, *135*, 6061–6068. [CrossRef]
50. Schumman, J.; Eichelbaum, M.; Lunkebein, T.; Thomas, N.; Álvarez Galván, M.C.; Schlögl, R.; Behrens, M. Promoting Strong Metal Support Interaction: Doping ZnO for Enhanced Activity of Cu/ZnO:M (M = Al, Ga, Mg) Catalysts. *ACS Catal.* **2015**, *5*, 3260–3270. [CrossRef]
51. Kornas, A.; Grabowski, R.; Śliwa, M.; Samson, K.; Ruggiero-Mikołajczyk, M.; Żelazny, M.A. Dimethyl ether synthesis from CO_2 hydrogenation over hybrid catalysts: Effects of preparation methods. *React. Kinet. Mech. Catal.* **2017**, *121*, 317–327. [CrossRef]
52. Li, M.M.J.; Zeng, Z.; Liao, F.; Hong, X.; Tsang, S.C.E. Enhanced CO_2 hydrogenation to methanol over CuZn nanoalloy in Ga modified Cu/ZnO catalysts. *J. Catal.* **2016**, *343*, 157–167. [CrossRef]
53. Guil-López, R.; Mota, N.; Llorente, J.; Millán, E.; Pawelec, B.; García, R.; Fierro, J.L.G.; Navarro, R.M. Structure and activity of Cu/ZnO catalysts co-modified with aluminium and gallium for methanol synthesis. *Catal. Today* **2020**, *355*, 870–881. [CrossRef]

54. Chen, W.H.; Lin, B.J.; Lee, H.M.; Huang, M.H. One-step synthesis of dimethyl ether from the gas mixture containing CO_2 with high space velocity. *Appl. Energy* **2012**, *98*, 92–101. [CrossRef]
55. Zhang, Y.J.; Li, D.B.; Jiang, D.; Zhu, Y.; Wu, Y.; Zhang, S.J.; Wang, K.J.; Wu, J. Effect of Mn promoter on structure and properties of Mn modified CuO–ZnO–ZrO_2/HZSM-5 catalysts for synthesis of dimethyl ether from CO_2 hydrogenation. *J. Mol. Catal.* **2014**, *28*, 344–350.
56. Meshkini, F.; Taghizadeh, M.; Bahmani, M. Investigating the effect of metal oxide additives on the properties of Cu/ZnO/Al_2O_3 catalysts in methanol synthesis from syngas using factorial experimental design. *Fuel* **2010**, *89*, 170–175. [CrossRef]
57. Yang, Y.; White, M.G.; Liu, P. Theoretical study of methanol synthesis from CO_2 hydrogenation on metal-doped Cu(111) surfaces. *J. Phys. Chem. C* **2012**, *116*, 248–256. [CrossRef]
58. Liu, L.; Fan, F.; Bai, M.; Xue, F.; Ma, X.; Jiang, Z.; Fang, T. Mechanistic study of methanol synthesis from CO_2 hydrogenation on Rh-doped Cu(111) surface. *Mol. Catal.* **2019**, *466*, 26–36. [CrossRef]
59. Pasupulety, N.; Driss, H.; Alhamed, Y.A.; Alzahrani, A.A.; Daous, M.A.; Petrov, L. Influence of preparation method on the catalytic activity of Au/Cu-Zn-Al catalysts for CO_2 hydrogenation to methanol. *Comptes Rendus Acad. Bulg. Sci.* **2015**, *68*, 1511–1518.
60. Melián-Cabrera, I.; López Granados, M.; Fierro, J.L.G. Pd-modified Cu–Zn catalysts for methanol synthesis from CO_2/H_2 mixtures: Catalytic structures and performance. *J. Catal.* **2002**, *210*, 285–294. [CrossRef]
61. Angelo, L.; Kobl, K.; Martínez-Tejada, L.M.; Zimmermann, Y.; Parkhomenko, K.; Roger, A.C. Study of CuZnMOx oxides (M = Al, Zr, Ce, CeZr) for the catalytic hydrogenation of CO_2 into methanol. *Comptes. Rendus. Chim.* **2015**, *18*, 250–260. [CrossRef]
62. Dong, X.; Li, F.; Zhao, N.; Xiao, F.; Wang, J.; Tan, Y. CO_2 hydrogenation to methanol over Cu/ZnO/ZrO_2 catalysts prepared by precipitation-reduction method. *Appl. Catal. B Environ.* **2016**, *191*, 8–17. [CrossRef]
63. Ateka, A.; Sierra, I.; Ereña, J.; Bilbao, J.; Aguayo, A.T. Performance of CuO–ZnO–ZrO_2 and CuO–ZnO–MnO as metallic functions and SAPO-18 as acid function of the catalyst for the synthesis of DME co-feeding CO_2. *Fuel Proc. Technol.* **2016**, *152*, 34–45. [CrossRef]
64. Frusteri, F.; Cordaro, M.; Cannilla, C.; Bonura, G. Multifunctionality of Cu-ZnO-ZrO_2/H-ZSM5 catalysts for the one-step CO_2-to-DME hydrogenation reaction. *Appl. Catal. B Environ.* **2015**, *162*, 57–65. [CrossRef]
65. Frusteri, F.; Bonura, G.; Cannilla, C.; Drago Ferrante, G.; Aloise, A.; Catizzone, E.; Migliori, M.; Giordano, G. Stepwise tuning of metal-oxide and acid sites of CuZnZr-MFI hybrid catalysts for the direct DME synthesis by CO_2 hydrogenation. *Appl. Catal. B Environ.* **2015**, *176–177*, 522–531. [CrossRef]
66. Mureddu, M.; Ferrara, F.; Pettinau, A. Highly efficient CuO/ZnO/ZrO_2@SBA-15 nanocatalysts for methanol synthesis from the catalytic hydrogenation of CO_2. *Appl. Catal. B Environ.* **2019**, *258*, 117941. [CrossRef]
67. Prieto, G.; Zečević, J.; Friedrich, H.; de Jong, K.P.; de Jongh, P.E. Towards stable catalysts by controlling collective properties of supported metal nanoparticles. *Nat. Mater.* **2013**, *12*, 34–39. [CrossRef]
68. Zhang, B.; Chen, Y.; Li, J.; Pippel, E.; Yang, H.; Gao, Z.; Qin, Y. High efficiency Cu-ZnO hydrogenation catalyst: The tailoring of Cu-ZnO interface sites by molecular layer deposition. *ACS Catal.* **2015**, *5*, 5567–5573. [CrossRef]
69. Deerattrakul, V.; Puengampholsrisook, P.; Limphirat, W.; Kongkachuichay, P. Characterization of supported Cu-Zn/graphene aerogel catalyst for direct CO_2 hydrogenation to methanol: Effect of hydrothermal temperature on graphene aerogel synthesis. *Catal. Today* **2018**, *314*, 154–163. [CrossRef]
70. Zhang, C.; Liao, P.; Wang, H.; Sun, J.; Gao, P. Preparation of novel bimetallic CuZn-BTC coordination polymer nanorod for methanol synthesis from CO_2 hydrogenation. *Mater. Chem. Phys.* **2018**, *215*, 211–220. [CrossRef]
71. Xiao, J.; Mao, D.; Guo, X.; Yu, J. Methanol synthesis from CO_2 hydrogenation over CuO-ZnO-TiO_2 catalysts: The influence of TiO_2 content. *Energy Technol.* **2015**, *3*, 32–39. [CrossRef]
72. Xu, J.H.; Su, X.; Liu, X.Y.; Pan, X.L.; Pei, G.X.; Huang, Y.Q.; Wang, X.D.; Zhang, T.; Geng, H.R. Methanol synthesis from CO_2 and H_2 over Pd/ZnO/Al_2O_3: Catalyst structure dependence of methanol selectivity. *Appl. Catal. A* **2016**, *514*, 51–59. [CrossRef]
73. Rui, N.; Wang, Z.Y.; Sun, K.H.; Ye, J.Y.; Ge, Q.F.; Liu, C.J. CO_2 hydrogenation to methanol over Pd/In_2O_3: Effects of Pd and oxygen vacancy. *Appl. Catal. B Environ.* **2017**, *218*, 488–497. [CrossRef]
74. Wu, C.Y.; Zhang, P.; Zhang, Z.F.; Zhang, L.J.; Yang, G.Y.; Han, B.X. Efficient hydrogenation of CO_2 to methanol over supported subnanometer gold catalysts at low temperature. *ChemCatChem* **2017**, *9*, 3691–3696. [CrossRef]
75. Zhong, J.; Yang, X.; Wu, Z.; Liang, B.; Huang, Y.; Zhanga, T. State of the art and perspectives in heterogeneous catalysis of CO_2 hydrogenation to methanol. *Chem. Soc. Rev.* **2020**, *49*, 1385–1413. [CrossRef] [PubMed]
76. Lian, Y.; Fang, T.F.; Zhang, Y.H.; Liu, B.; Li, J.L. Hydrogenation of CO_2 to alcohol species over Co@Co_3O_4/C-N catalysts. *J. Catal.* **2019**, *379*, 46–51. [CrossRef]
77. Li, C.S.; Melaet, G.; Ralston, W.T.; An, K.; Brooks, C.; Ye, Y.F.; Liu, Y.S.; Zhu, J.F.; Guo, J.H.; Alayoglu, S.; et al. High-performance hybrid oxide catalyst of manganese and cobalt for low-pressure methanol synthesis. *Nat. Commun.* **2015**, *6*, 6538. [CrossRef]
78. Hanseul Choi, Sunyoung Oh, Si Bui Trung Tran, Jeong Young Park, Size-controlled model Ni catalysts on Ga_2O_3 for CO_2 hydrogenation to methanol. *J. Catal.* **2019**, *376*, 68–76. [CrossRef]
79. Sun, K.H.; Fan, Z.G.; Ye, J.Y.; Yan, J.M.; Ge, Q.F.; Li, Y.N.; He, W.J.; Yang, W.; Liu, C.J. Hydrogenation of CO_2 to methanol over In_2O_3 catalyst. *J. CO_2. Util.* **2015**, *12*, 1–6. [CrossRef]

80. Martin, O.; Martin, A.J.; Mondelli, C.; Mitchell, S.; Segawa, T.F.; Hauert, R.; Drouilly, C.; Curulla-Ferré, D.; Pérez-Ramírez, J. Indium oxide as a superior catalyst for methanol synthesis by CO_2 hydrogenation. *Angew. Chem. Int. Ed.* **2016**, *55*, 6261–6265. [CrossRef] [PubMed]
81. Chen, T.Y.; Cao, C.X.; Chen, T.B.; Ding, X.X.; Huang, H.; Shen, L.; Cao, X.Y.; Zhu, M.H.; Xu, J.; Gao, J.; et al. Unraveling highly tunable selectivity in CO_2 hydrogenation over bimetallic In-Zr oxide catalysts. *ACS Catal.* **2019**, *9*, 8785–8797. [CrossRef]
82. Frei, M.S.; Mondelli, C.; Cesarini, A.; Krumeich, F.; Hauert, R.; Stewart, J.A.; Ferre, D.C.; Perez-Ramirez, J. Role of Zirconia in Indium Oxide-Catalyzed CO_2 Hydrogenation to Methanol. *ACS Catal.* **2020**, *10*, 1133–1145. [CrossRef]
83. Akkharaphatthawona, N.; Chanlekc, N.; Cheng, C.K.; Chareonpanicha, M.; Limtrakule, J.; Witoon, T. Tuning adsorption properties of $Ga_xIn_{2-x}O_3$ catalysts for enhancement of methanol synthesis activity from CO_2 hydrogenation at high reaction temperature. *Appl. Surf. Sci.* **2019**, *489*, 278–286. [CrossRef]
84. Studt, F.; Sharafutdinov, I.; Abild-Pedersen, F.; Elkjaer, C.F.; Hummelshoj, J.S.; Dahl, S.; Chorkendorff, I.; Norskov, J.K. Discovery of a Ni-Ga catalyst for carbon dioxide reduction to methanol. *Nat. Chem.* **2014**, *6*, 320–324. [CrossRef]
85. Pustovarenko, A.; Dikhtiarenko, A.; Bavykina, A.; Gevers, L.; Ramírez, A.; Russkikh, A.; Telalovic, S.; Aguilar, A.; Hazemann, J.-L.; Ould-Chikh, S.; et al. Metal–organic framework-derived synthesis of cobalt indium catalysts for the hydrogenation of CO_2 to methanol. *ACS Catal.* **2020**, *10*, 5064–5076. [CrossRef]
86. Richard, A.R.; Fan, M. The effect of lanthanide promoters on NiInAl/SiO_2 catalyst for methanol synthesis. *Fuel* **2018**, *222*, 513–522. [CrossRef]
87. Akarmazyan, S.S.; Panagiotopoulou, P.; Kambolis, A.; Papadopoulou, C.; Kondarides, D.I. Methanol dehydration to dimethyl ether over Al_2O_3 catalysts. *Appl. Catal. B Environ.* **2014**, *145*, 136–148. [CrossRef]
88. Osman, A.I.; Abu-Dahrieh, J.K.; Rooney, D.W.; Thompson, J.; Halawy, S.A.; Mohamed, M.A. Surface hydrophobicity and acidity effect on alumina catalyst in catalytic methanol dehydration reaction. *J. Chem. Technol. Biotechnol.* **2017**, *92*, 2952–2962. [CrossRef]
89. Raoof, F.; Taghizadeh, M.; Eliassi, A.; Yaripour, F. Effects of temperature and feed composition on catalytic dehydration of methanol to dimethyl ether over γ-alumina. *Fuel* **2008**, *87*, 2967–2971. [CrossRef]
90. Bateni, H.; Able, C. Development of heterogeneous catalysts for dehydration of methanol to dimethyl ether: A review. *Catal. Ind.* **2019**, *11*, 7–33. [CrossRef]
91. Ghorbanpour, A.; Rimer, J.D.; Grabow, L.C. Computational assessment of the dominant factors governing the mechanism of methanol dehydration over H-ZSM-5 with heterogeneous aluminum distribution. *ACS Catal.* **2016**, *6*, 2287–2298. [CrossRef]
92. Jones, J.A.; Iglesia, E. Kinetic, spectroscopic, and theroretical assessment of associative and dissociative metanol dehydration routes in zeolites. *Angew. Chem. Int. Ed.* **2014**, *53*, 12177–12181. [CrossRef]
93. Hosseininejad, S.; Afacan, A.; Hayes, R.E. Catalytic and kinetic study of methanol dehydration to dimethyl ether. *Chem. Eng. Res. Des.* **2012**, *90*, 825–833. [CrossRef]
94. Osman, A.I.; Abu-Dahrieh, J.K. Kinetic investigation of η-Al_2O_3 catalyst for dimethyl ether production. *Catal. Lett.* **2018**, *148*, 1236–1245. [CrossRef]
95. Osman, A.I.; Abu-Dahrieh, J.K.; Rooney, D.W.; Halawy, S.A.; Mohamed, M.A.; Abdelkader, A. Effect of precursor on the performance of alumina for the dehydration of methanol to dimethyl ether. *Appl. Catal. B* **2012**, *127*, 307–315. [CrossRef]
96. Kim, S.M.; Lee, Y.J.; Bae, J.W.; Potdar, H.S.; Jun, K.W. Synthesis and characterization of a highly active alumina catalyst for methanol dehydration to dimethyl ether. *Appl. Catal. A Gen.* **2008**, *348*, 113–120. [CrossRef]
97. Carvalho, D.F.; Almeida, G.C.; Monteiro, R.S.; Mota, C.J.A. Hydrogenation of CO_2 to Methanol and Dimethyl Ether over a Bifunctional Cu·ZnO Catalyst Impregnated on Modified γ-Alumina. *Energy Fuels* **2020**, *34*, 7269–7274. [CrossRef]
98. Yaripour, F.; Shariatinia, Z.; Sahebdelfar, S.; Irandoukht, A. The effects of synthesis operation conditions on the properties of modified-alumina nanocatalysts in methanol dehydration to dimethyl ether using factorial experimental design. *Fuel* **2015**, *139*, 40–50. [CrossRef]
99. Chiang, C.-L.; Lin, K.-S. Preparation and characterization of CuO/Al_2O_3 catalyst for dimethyl ether production via methanol dehydration. *Inter. J. Hydrog. Energy* **2017**, *42*, 23526–23538. [CrossRef]
100. Armenta, M.A.; Valdez, R.; Quintana, J.M.; Silva-Rodrigo, R.; Cota, L.; Olivas, A. Highly selective CuO/γ-Al_2O_3 catalyst promoted with hematite for efficient methanol dehydration to dimethyl ether. *Inter. J. Hydrog. Energy* **2018**, *43*, 6551–6560. [CrossRef]
101. Armenta, M.A.; Maytorena, V.M.; Flores–Sánchez, L.A.; Quintana, J.M.; Valdez, R.; Olivas, A. Dimethyl ether production via methanol dehydration using Fe_3O_4 and CuO over γ-χ- Al_2O_3 nanocatalysts. *Fuel* **2020**, *280*, 118545. [CrossRef]
102. Catizzone, E.; Aloise, A.; Migliori, M.; Giordano, G. Dimethyl ether synthesis via methanol dehydration: Effect of zeolite structure. *Appl. Catal. A Gen.* **2015**, *502*, 215–220. [CrossRef]
103. Catizzone, E.; Aloise, A.; Migliori, M.; Giordano, G. From 1-D to 3-D zeolite structures: Performance assessment in catalysis of vapour-phase methanol dehydration to DME. *Microp. Mesopo. Mat.* **2017**, *243*, 102–111. [CrossRef]
104. Frusteri, F.; Migliori, M.; Cannilla, C.; Frusteri, L.; Catizzone, E.; Aloise, A.; Giordano, G.; Bonura, G. Direct CO_2-to-DME hydrogenation reaction: New evidences of a superior behavior of FER-based hybrid systems to obtain high DME yield. *J. CO_2 Util.* **2017**, *18*, 353–361. [CrossRef]
105. Dębek, R.; Ribeiro, M.F.G.; Fernandes, A.; Motak, M. Dehydration of methanol to dimethyl ether over modified vermiculites. *C. R. Chim.* **2015**, *18*, 1211e22. [CrossRef]

106. Cai, M.; Palčić, A.; Subramanian, V.; Moldovan, S.; Ersen, O.; Valtchev, V.; Ordomsky, V.V.; Khodakov, A.Y. Direct Dimethyl Ether Synthesis from Syngas on Copper-Zeolite Hybrid Catalysts with a Wide Range of Zeolite Particle Sizes. *J. Catal.* **2016**, *338*, 227. [CrossRef]
107. Aboul-Fotouh, S.M.K.; Ali, L.I.; Naghmash, M.A.; Aboul-Gheit, N.A.K. Effect of the Si/Al ratio of HZSM-5 zeolite on the production of dimethyl ether before and after ultrasonication. *J. Fuel Chem. Technol.* **2017**, *45*, 581–588. [CrossRef]
108. Aboul-Fotouh, S.M.K.; Aboul-Gheit, N.A.K.; Hassan, M.M.I. Conversion of methanol using modified H-MOR zeolite catalysts. *Chin. J. Catal.* **2011**, *32*, 412–417. [CrossRef]
109. Aboul-Fotouh, S.M.K.; Aboul-Gheit, N.A.K.; Naghmash, M.A. Dimethylether production on zeolite catalysts activated by Cl^-, F^- and/or ultrasonication. *J. Fuel Chem. Technol.* **2016**, *44*, 428–436. [CrossRef]
110. Aloise, A.; Marino, A.; Dalena, F.; Giorgianni, G.; Migliori, M.; Frusteri, L.; Cannilla, C.; Bonura, G.; Frusteri, F.; Giordano, G. Desilicated ZSM-5 zeolite: Catalytic performances assessment in methanol to DME dehydration. *Micropor. Mesopor. Mat.* **2020**, *302*, 110198. [CrossRef]
111. Dennis-Smither, B.J.; Yang, Z.; Buda, C.; Liu, X.; Sainty, N.; Tanb, X.; Sunley, G.J. Getting zeolite catalysts to play your tune: Methyl carboxylate esters as switchable promoters for methanol dehydration to DME. *Chem. Commun.* **2019**, *55*, 13804. [CrossRef] [PubMed]
112. Magzoub, F.; Li, X.; Lawson, S.; Rezaei, F.; Rownaghi, A.A. 3D-printed HZSM-5 and 3D-HZM5@SAPO-34 structured monoliths with controlled acidity and porosity for conversion of methanol to dimethyl ether. *Fuel* **2020**, *280*, 118628. [CrossRef]
113. Catizzone, E.; Bonura, G.; Migliori, M.; Braccio, G.; Frusteri, F.; Giordano, G. Direct CO_2-to-dimethyl ether hydrogenation over CuZnZr/zeolite hybrid catalyst: New evidence on the interaction between acid and metal sites. *Ann. Chim. Sci. Mat.* **2019**, *43*, 141–149. [CrossRef]
114. Solyman, S.M.; Aboul-Gheit, N.A.K.; Sadek, M.; Tawfik, F.M.; Ahmed, H.A. The effect of physical and chemical treatment on nano-zeolite characterization and their performance in dimethyl ether preparation. *Egypt. J. Pet.* **2015**, *24*, 289–297. [CrossRef]
115. Micek-Ilnicka, A. The role of water in the catalysis on solid heteropolyacids. *J. Mol. Catal. A Chem.* **2009**, *308*, 1–14. [CrossRef]
116. Schnee, J.; Gaigneaux, E.M. Elucidating and exploiting the chemistry of keggin heteropolyacids in the methanol-to-dme conversion: Enabling the bulk reaction thanks to operando raman. *Catal. Sci. Technol.* **2017**, *7*, 817–830. [CrossRef]
117. Schnee, J.; Eggermont, A.; Gaigneaux, E.M. Boron nitride: A support for highly active heteropolyacids in the methanol-to-dme reaction. *ACS Catal.* **2017**, *7*, 4011–4017. [CrossRef]
118. Ladera, R.M.; Ojeda, M.; Fierro, J.L.G.; Rojas, S. Tio2-supported heteropoly acid catalysts for dehydration of methanol to dimethyl ether: Relevance of dispersion and support interaction. *Catal. Sci. Technol.* **2015**, *5*, 484–491. [CrossRef]
119. García-López, E.I.; Marcì, G.; Krivtsov, I.; Casado Espina, J.; Liotta, L.F.; Serrano, A. Local structure of supported keggin and wells–dawson heteropolyacids and its influence on the catalytic activity. *J. Phys. Chem.* **2019**, *123*, 19513–19527. [CrossRef]
120. Alharbi, W.; Kozhevnikova, E.F.; Kozhevnikov, I.V. Dehydration of methanol to dimethyl ether over heteropoly acid catalysts: The relationship between reaction rate and catalyst acid strength. *ACS Catal.* **2015**, *5*, 7186–7193. [CrossRef]
121. Peinado, C.; Liuzzi, D.; Ladera-Gallardo, R.M.; Retuerto, N.; Ojeda, M.; Peña, M.A.; Rojas, S. Effects of support and reaction pressure for the synthesis of dimethyl ether over heteropolyacid catalysts. *Sci. Rep.* **2020**, *10*, 8551. [CrossRef] [PubMed]
122. Millán, E.; Mota, N.; Guil-López, R.; Pawelec, B.; Fierro, J.L.G.; Navarro, R.M. Bifunctional Hybrid Catalysts Based on Supported $H_3PW_{12}O_{40}$ and Cu-ZnO(Al): Effect of Heteropolyacid Loading on Hybrid Structure and Catalytic Activity. *Catalysts* **2020**, *10*, 1071. [CrossRef]
123. Ladera, R.M.; Fierro, J.L.G.; Ojeda, M.; Rojas, S. TiO_2-supported heteropoly acids for low-temperature synthesis of dimethyl ether from methanol. *J. Catal.* **2014**, *312*, 195–203. [CrossRef]
124. Kornas, A.; Śliwa, M.; Ruggiero-Mikołajczyk, M.; Samson, K.; Podobiński, J.; Karcz, R.; Duraczyńska, D.; Rutkowska-Zbik, D.; Grabowski, R. Direct hydrogenation of CO_2 to dimethyl ether (DME) over hybrid catalysts containing CuO/ZrO_2 as a metallic function and heteropolyacids as an acidic function. *Reac. Kinet. Mech. Cat.* **2020**, *130*, 179–194. [CrossRef]
125. Yu, Y.; Sun, D.; Wang, S.; Xiao, M.; Sun, L.; Meng, Y. Heteropolyacid Salt Catalysts for Methanol Conversion to Hydrocarbons and Dimethyl Ether: Effect of Reaction Temperature. *Catalysts* **2019**, *9*, 320. [CrossRef]
126. Chen, Z.; Li, X.; Xu, Y.; Dong, Y.; Lai, W.; Fang, W.; Yi, X. Fabrication of nano-sized SAPO-11 crystals with enhanced dehydration of methanol to dimethyl ether. *Catal. Commun.* **2018**, *103*, 1–4. [CrossRef]
127. Sánchez-Contador, M.; Ateka, A.; Aguayo, A.T.; Bilbao, J. Behavior of SAPO-11 as acid function in the direct synthesis of dimethyl ether from syngas and CO_2. *J. Ind. Eng. Chem.* **2018**, *63*, 245–254. [CrossRef]
128. Pranee, W.; Neramittagapong, S.; Assawasaengrat, P.; Neramittagapong, A. Methanol dehydration to dimethyl ether over strong-acid-modified diatomite catalysts. *Energy Sources Part A Recovery Util. Environ. Eff.* **2016**, *38*, 3109–3115. [CrossRef]
129. Temvuttirojn, C.; Chuasomboon, N.; Numpilai, T.; Faungnawakij, K.; Chareonpanich, M.; Limtrakul, J.; Witoon, T. Development of SO_4^{2-}–ZrO_2 acid catalysts admixed with a CuO-ZnO-ZrO_2 catalyst for CO_2 hydrogenation to dimethyl ether. *Fuel* **2019**, *241*, 695–703. [CrossRef]
130. Witoon, T.; Permsirivanich, T.; Kanjanasoontorn, N.; Akkaraphataworn, C.; Seubsai, A.; Faungnawakij, K.; Warakulwit, C.; Chareonpanich, M.; Limtrakul, J. Direct synthesis of dimethyl ether from CO_2 hydrogenation over cu-ZnO-ZrO_2/SO_4^{2-}-ZrO_2 hybrid catalysts: Effects of sulfur-to-zirconia ratios. *Catal. Sci. Technol.* **2015**, *5*, 2347–2357. [CrossRef]

131. Suwannapichat, Y.; Numpilai, T.; Chanlek, N.; Faungnawakij, K.; Chareonpanich, M.; Witoon, T. Direct synthesis of dimethyl ether from CO_2 hydrogenation over novel hybrid catalysts containing a Cu-ZnO-ZrO_2 catalyst admixed with WO_x/Al_2O_3 catalysts: Effects of pore size of Al_2O_3 support and W loading content. *Energy Convers. Manag.* **2018**, *159*, 20–29. [CrossRef]
132. Witoon, T.; Kachaban, N.; Donphai, W.; Kidkhunthod, P.; Faungnawakij, K.; Chareonpanich, M.; Limtrakul, J. Tuning of catalytic CO_2 hydrogenation by changing composition of CuO-ZnO-ZrO_2 catalysts. *Energy Convers. Manag.* **2016**, *118*, 21–31. [CrossRef]
133. Macht, J.; Baertsch, C.D.; May-Lozano, M.; Soled, S.L.; Wang, Y.; Iglesia, E. Support effects on Brønsted acid site densites and alcohol dehydration turnover rates on tungsten oxide domians. *J. Catal.* **2004**, *227*, 479–491. [CrossRef]
134. Ladera, R.M.; Finocchio, E.; Rojas, S.; Busca, G.; Fierro, J.L.G.; Ojeda, M. Supported WOx-based catalysts for methanol dehydration to dimethyl ether. *Fuel* **2013**, *113*, 1–9. [CrossRef]
135. Ladera, R.M.; Finocchio, E.; Rojas, S.; Fierro, J.L.G.; Ojeda, M. Supported niobium catalysts for methanol dehydration to dimethyl ether: FTIR studies of acid properties. *Catal. Today* **2012**, *192*, 136–143. [CrossRef]
136. Bonura, G.; Cordaro, M.; Spadaro, L.; Cannilla, C.; Arena, F.; Frusteri, F. Hybrid Cu-ZnO-ZrO_2/H-ZSM-5 system for the direct synthesis of DME by CO_2 hydrogenation. *Appl. Catal. B Environ.* **2013**, *140–141*, 16–24. [CrossRef]
137. Bonura, G.; Cordaro, M.; Cannilla, C.; Arena, F.; Frusteri, F. The changing nature of the active site of Cu-Zn-Zr catalysts for the CO_2 hydrogenation reaction to methanol. *Appl. Catal. B Environ.* **2014**, *152–153*, 152–161. [CrossRef]
138. Bonura, G.; Frusteri, F.; Cannilla, C.; Drago Ferrante, G.; Aloise, A.; Catizzone, E.; Migliori, M.; Giordano, G. Catalytic features of CuZnZr–zeolite hybrid systems for the direct CO_2-to-DME hydrogenation reaction. *Catal. Today* **2016**, *277*, 48–54. [CrossRef]
139. Zhang, Y.; Zhang, Y.; Ding, F.; Wang, K.; Wang, X.; Ren, B.; Wu, J. Synthesis of DME by CO_2 hydrogenation over La_2O_3-modified CuO-ZnO-ZrO_2/HZSM-5 catalysts. *Chem. Ind. Chem. Eng. Q.* **2017**, *23*, 49–56. [CrossRef]
140. Guo, X.; Mao, D.; Lu, G.; Wang, S.; Wu, G. The influence of La doping on the catalytic behavior of Cu/ZrO_2 for methanol synthesis from CO_2 hydrogenation. *J. Mol. Catal. A Chem.* **2011**, *345*, 60–68. [CrossRef]
141. Jeong, C.; Park, J.; Kim, J.; Baik, J.H.; Suh, Y.-W. Effects, of Al^{3+} precipitation onto primitive amorphous Cu-Zn precipitate on methanol synthesis over Cu/ZnO/Al_2O_3 catalyst. *Korean J. Chem. Eng.* **2019**, *36*, 191–196. [CrossRef]
142. Jiang, Q.; Liu, Y.; Dintzer, T.; Luo, J.; Parkhomenko, K.; Roger, A. Tuning the highly dispersed metallic cu species via manipulating Brønsted acid sites of mesoporous aluminosilicate support for CO_2 hydrogenation reactions. *Appl. Catal. B Environ.* **2020**, *269*, 118804. [CrossRef]
143. Lu, S.; Si, B.; Chang, Q.; Liu, B.; Liu, E.; Fan, J. Modification of the CuO-ZnO-Al_2O_3/HZSM-5 bifunctional catalyst with promoters and their catalytic performance research. *Huaxue Gongcheng/Chem. Eng.* **2016**, *44*, 42–47. [CrossRef]
144. Qin, Z.-Z.; Zhou, X.-H.; Su, T.-M.; Jiang, Y.-X.; Ji, H.-B. Hydrogenation of CO_2 to dimethyl ether on La-, Ce-modified Cu-Fe/HZSM-5 catalysts. *Catal. Commun.* **2016**, *75*, 78–82. [CrossRef]
145. Bao, J.; Tsubaki, N. Design and synthesis of powerful capsule catalysts aimed at applications in C1 chemistry and biomass conversion. *Chem. Rec.* **2018**, *18*, 4–19. [CrossRef]
146. Gao, X.H.; Ma, Q.X.; Zhao, T.S.; Bao, J.; Tsubaki, N. Recent advances in multifunctional capsule catalysts in heterogeneous catalysis. *Chin. J. Chem. Phys.* **2018**, *31*, 393–403. [CrossRef]
147. Yang, G.; Tsubaki, N.; Shamoto, J.; Yoneyama, Y.; Zhang, Y. Confinement effect and synergistic function of H-ZSM-5/Cu-ZnO-Al_2O_3 capsule catalyst for one-step controlled synthesis. *J. Am. Chem. Soc.* **2010**, *132*, 8129–8136. [CrossRef]
148. Yang, G.; Wang, D.; Yoneyama, Y.; Tan, Y.; Tsubaki, N. Facile synthesis of H-type zeolite shell on a silica substrate for tandem catalysis. *Chem. Commun.* **2012**, *48*, 1263–1265. [CrossRef] [PubMed]
149. Phienluphon, R.; Pinkaew, K.; Yang, G.; Li, J.; Wei, Q.; Yoneyama, Y.; Vitidsant, T.; Tsubaki, N. Designing core (Cu/ZnO/Al_2O_3)-shell (SAPO-11) zeolite capsule catalyst with a facile physical way for dimethyl ether direct synthesis from syngas. *Chem. Eng. J.* **2015**, *270*, 605–611. [CrossRef]
150. Tan, L.; Zhang, P.; Suzuki, Y.; Li, H.; Guo, L.; Yoneyama, Y.; Chen, J.; Peng, X.; Tsubaki, N. Bifunctional capsule catalyst of Al_2O_3@Cu with strengthened dehydration reaction field for direct synthesis of dimethyl ether from syngas. *Ind. Eng. Chem. Res.* **2019**, *58*, 51, 22905–22911. [CrossRef]
151. Atakan, A.; Keraudy, J.; Mäkie, P.; Hulteberg, C.; Björk, E.M.; Odén, M. Impact of the morphological and chemical properties of copper-zirconium-SBA-15 catalysts on the conversion and selectivity in carbon dioxide hydrogenation. *J. Colloid Interface Sci.* **2019**, *546*, 163–173. [CrossRef]
152. Bahruji, H.; Amstrong, R.D.; Ruiz Esquius, J.; Jones, W.; Bowker, M.; Hutchings, G.J. Hydrogenation of CO_2 to Dimethyl Ether over Brønsted Acidic PdZn Catalysts. *Ind. Eng. Chem. Res.* **2018**, *57*, 6821–6829. [CrossRef]
153. Ahoba-Sam, C.; Borfecchia, E.; Lazzarini, A.; Bugaev, A.; Adamu Isah, A.; Taoufik, M.; Bordiga, S.; Olsbye, U. On the conversion of CO_2 to value added products over composite PdZn and H-ZSM-5 catalysts: Excess Zn over Pd, a compromise or a penalty? *Catal. Sci. Technol.* **2020**, *10*, 4373–4385. [CrossRef]
154. Zhang, Y.J.; Li, D.B.; Zhang, S.J.; Wang, K.J.; Wu, J. CO_2 hydrogenation to dimethyl ether over CuO–ZnO–Al_2O_3/HZSM-5 prepared by combustion route. *RSC Adv.* **2014**, *4*, 16391–16396. [CrossRef]
155. Ren, S.; Fan, X.; Shang, Z.; Shoemaker, W.R.; Ma, L.; Wu, T.; Li, S.; Klinghoffer, N.B.; Yu, M.; Liang, X. Enhanced catalytic performance of Zr modified CuO/ZnO/Al_2O_3 catalyst for methanol and DME synthesis via CO_2 hydrogenation. *J. CO2 Util.* **2020**, *36*, 82–95. [CrossRef]
156. Hu, Y.; Zhang, Y.; Du, J.; Li, C.; Wang, K.; Liu, L.; Yu, X.; Wang, K.; Li, N. The influence of composition on the functionality of hybrid CuO–ZnO–Al_2O_3/HZSM-5 for the synthesis of DME from CO_2 hydrogenation. *RSC Adv.* **2018**, *8*, 30387–30395. [CrossRef]

157. Li, L.Y.; Mao, D.S.; Xiao, J.; Li, L.; Guo, X.M.; Yu, J. Facile preparation of highly efficient CuO-ZnO-ZrO_2/HZSM-5 bifunctional catalyst for one-step CO_2 hydrogenation to dimethyl ether: Influence of calcination temperature. *Chem. Eng. Res. Des.* **2016**, *111*, 100–108. [CrossRef]
158. Bonura, G.; Cannilla, C.; Frusteri, L.; Frusteri, F. The influence of different promoter oxides on the functionality of hybrid CuZn-ferrierite systems for the production of DME from CO_2-H_2 mixtures. *Appl. Catal. A Gen.* **2017**, *544*, 21–29. [CrossRef]
159. Miletto, I.; Catizzone, E.; Bonura, G.; Ivaldi, C.; Migliori, M.; Gianotti, E.; Marchese, L.; Frusteri, F.; Giordano, G. In situ FT-IR characterization of CuZnZr/ferrierite hybrid catalysts for one-pot CO2-to-DME conversion. *Materials* **2018**, *11*, 2275. [CrossRef] [PubMed]